OPEN ACCESS

Repository of the Max Delbrück Center for Molecular Medicine (MDC) in the Helmholtz Association

https://edoc.mdc-berlin.de/20419/

Skin sodium accumulates in psoriasis and reflects disease severity

Maifeld A., Wild J., Karlsen T.V., Rakova N., Wistorf E., Linz P., Jung R., Birukov A., Gimenez-Rivera V.A., Wilck N., Bartolomaeus T., Dechend R., Kleinewietfeld M., Forslund S.K., Krause A., Kokolakis G., Philipp S., Clausen B.E., Brand A., Waisman A., Kurschus F.C., Wegner J., Schultheis M., Luft F.C., Boschmann M., Kelm M., Wiig H., Kuehne T., Müller D.N., Karbach S., Markó L.

This is the final version of the accepted manuscript. The original article has been published in final edited form in:

Journal of Investigative Dermatology
2022 JAN ; 142(1): 166-178
2021 JUL 06 (first published online: final publication)
doi: 10.1016/j.jid.2021.06.013

Publisher: Elsevier

Copyright © 2021 The Authors. Published by Elsevier, Inc. on behalf of the Society for Investigative Dermatology. This manuscript version is made available under the Creative Commons Attribution-NonCommercial-NoDerivatives 4.0 International License. To view a copy of this license, visit http://creativecommons.org/licenses/by-nc-nd/4.0/ or send a letter to Creative Commons, PO Box 1866, Mountain View, CA 94042, USA.

Skin Sodium Accumulates in Psoriasis and Reflects Disease Severity

András Maifeld[1,2,3,4]*, Johannes Wild[5,6]*, Tine V. Karlsen[7], Natalia Rakova[1], Elisa Wistorf[1], Peter Linz[8,9], Rebecca Jung[6,10], Anna Birukov[1,2,11,12], Vladimir-Andrey Gimenez-Rivera[13], Nicola Wilck[1,2,3,14], Theda Bartolomaeus[1,2,4], Ralf Dechend[1,2,3,4,15], Markus Kleinewietfeld[16], Sofia K. Forslund[1,2,3,4], Andreas Krause[17], Georgios Kokolakis[18], Sandra Philipp[18], Björn E. Clausen[9], Anna Brand[9], Ari Waisman[9], Florian C. Kurschus[19], Joanna Wegner[20], Michael Schultheis[20], Friedrich C. Luft[1], Michael Boschmann[1,3,4], Marcus Kelm[3,21,22], Helge Wiig[7], Titus Kuehne[21,22], Dominik N. Müller[1,2,3,4,23*], Susanne Karbach[5,6*], Lajos Markó[1,2,3,4*]

[1]Experimental and Clinical Research Center, a cooperation of Charité – Universitätsmedizin Berlin and Max Delbrück Center for Molecular Medicine, Berlin, Germany.

[2]DZHK (German Centre for Cardiovascular Research), partner site Berlin, Germany.

[3]Berlin Institute of Health at Charité - Universitätsmedizin Berlin, Berlin, Germany.

[4]Charité - Universitätsmedizin Berlin, corporate member of Freie Universität Berlin and Humboldt-Universität zu Berlin, Berlin, Germany.

[5]Center of Cardiology - Cardiology I, Johannes Gutenberg-University Mainz, Mainz, Germany.

[6]Center for Thrombosis and Hemostasis (CTH), Johannes Gutenberg-University Mainz, Mainz, Germany.

[7]Department of Biomedicine, University of Bergen, Norway.

[8]Institute of Radiology, Friedrich-Alexander-University Erlangen-Nürnberg, Erlangen, Germany.

[9]Department of Nephrology and Hypertension, Friedrich-Alexander-University Erlangen-Nürnberg, Erlangen, Germany

[10]Institute for Molecular Medicine, University Medical Center Mainz, Mainz, Germany.

[11]Department of Molecular Epidemiology, German Institute of Human Nutrition Potsdam-Rehbrücke, Nuthetal, Germany.

[12]German Center for Diabetes Research (DZD), München–Neuherberg, Germany.

[13]IntegraSkin GmbH i.G., Tübingen, Germany

[14]Charité - Universitätsmedizin Berlin, corporate member of Freie Universität Berlin and Humboldt-Universität zu Berlin, Department of Nephrology and Internal Intensive Care Medicine, Berlin, Germany

[15]Helios Clinic Berlin-Buch, Berlin, Germany.

[16]VIB Laboratory of Translational Immunomodulation, VIB Center for Inflammation Research (IRC), UHasselt, Campus Diepenbeek, Hasselt, Belgium.

[17]Immanuel Krankenhaus Berlin, Medical Centre for Rheumatology and Clinical Immunology, Berlin, Germany.

[18]Charité - Universitätsmedizin Berlin, corporate member of Freie Universität Berlin and Humboldt-Universität zu Berlin, Department of Dermatology, Venereology and Allergology, Berlin, Germany

[19]Department of Dermatology, Heidelberg University Hospital, Heidelberg, Germany

[20]Department of Dermatology, University Medical Center Mainz, Mainz, Germany

[21]Institute for Imaging Science and Computational Modelling in Cardiovascular Medicine, Charité - Universitätsmedizin Berlin, Berlin, Germany

[22]Department of Congenital Heart Disease, German Heart Center Berlin (Deutsches Herzzentrum Berlin, DHZB), Berlin, Germany.

[23]Max Delbrück Center for Molecular Medicine in the Helmholtz Association Berlin, Germany.

* These authors contributed equally to this work

Corresponding author: Lajos Markó, Experimental and Clinical Research Center, a cooperation of Charité - Universitätsmedizin Berlin and Max Delbrück Center for Molecular Medicine, Lindenberger Weg 80, 13125 Berlin, Germany. Phone: +49-30-450-540-144. Email: lajos.marko@charite.de.

Short title: Skin Sodium in Psoriasis

Abbreviations: IMQ, imiquimod; interleukin, IL; MRI, magnetic resonance imaging; PBMC, peripheral blood mononuclear cells; psoriasis area and severity index, PASI; T helper 17 cell, Th17; VEGFC, vascular endothelial growth factor C; VEGFR, vascular endothelial growth factor receptor.

ORCID ID List:

András Maifeld	orcid.org/0000-0001-8756-747X
Johannes Wild	orcid.org/0000-0002-1446-8101
Tine V. Karlsen	orcid.org/0000-0002-1512-2479
Natalia Rakova	orcid.org/0000-0002-5397-6715
Elisa Wistorf	orcid.org/0000-0002-5592-5743
Peter Linz	orcid.org/0000-0002-8232-1443
Rebecca Jung	orcid.org/0000-0002-2460-6512
Anna Birukov	orcid.org/0000-0002-8306-3351
Vladimir-Andrey Gimenez-Rivera	orcid.org/0000-0001-5055-208X
Nicola Wilck	orcid.org/0000-0003-3189-5364
Theda Bartolomaeus	orcid.org/0000-0002-5156-7184

Ralf Dechend	orcid.org/0000-0001-6636-3080
Markus Kleinewietfeld	orcid.org/0000-0002-2832-3149
Sofia K. Forslund	orcid.org/0000-0003-4285-6993
Andreas Krause	orcid.org/0000-0001-6000-2815
Georgios Kokolakis	orcid.org/0000-0002-8042-7885
Sandra Philipp	orcid.org/0000-0002-9421-5461
Björn E. Clausen	orcid.org/0000-0002-2484-7842
Anna Brand	orcid.org/0000-0002-3615-1826
Ari Waisman	orcid.org/0000-0003-4304-8234
Florian C. Kurschus	orcid.org/0000-0001-7550-0681
Joanna Wegner	orcid.org/0000-0002-7710-9675
Michael Schultheis	orcid.org/0000-0002-2957-074X
Friedrich C. Luft	orcid.org/0000-0002-8635-1199
Michael Boschmann	orcid.org/0000-0002-0114-7114
Marcus Kelm	orcid.org/0000-0003-4971-0452
Helge Wiig	orcid.org/0000-0002-7740-8210
Titus Kuehne	orcid.org/0000-0003-1631-4824
Dominik N. Müller	orcid.org/0000-0003-3650-5644
Susanne Karbach	orcid.org/0000-0003-4462-3747
Lajos Markó	orcid.org/0000-0003-1888-5575

ABSTRACT

Sodium can accumulate in the skin, at concentrations exceeding serum levels. High sodium environment can lead to pathogenic T helper (Th)17 cell expansion. Psoriasis is a chronic inflammatory skin disease in which interleukin (IL)-17-producing Th17 cells play a crucial role. In an observational study, we measured skin sodium content in psoriasis patients and age-matched healthy controls by ^{23}Na-magnetic resonance imaging (MRI). Patients with a psoriasis area and severity index (PASI)>5 showed significantly higher sodium and water content in the skin, but not in other tissues, compared to those with lower PASI or healthy controls. Skin sodium concentrations measured by ^{23}Na-spectroscopy or by atomic adsorption spectrometry in ashed-skin biopsies verified findings with ^{23}Na-MRI. *In vitro* Th17 cell differentiation of naïve $CD4^+$ cells from psoriatic patients markedly induced IL-17A expression under increased NaCl concentrations. The imiquimod-induced psoriasis mouse model replicated the human findings. Extracellular tracer ^{51}Cr-EDTA measurements in imiquimod- and sham-treated skin showed similar extracellular volumes, rendering excessive water of intracellular origin. Chronic genetic IL-17A-driven psoriasis mouse models underlined the role of IL-17A in dermal sodium accumulation and inflammation. Our data describe skin sodium as a pathophysiological feature of psoriasis, which could open new avenues for its treatment.

INTRODUCTION

Sodium is an essential mineral and osmolyte for the human body. It is the major cation in the extracellular fluid and as such plays a crucial role in homeostatic processes such as regulation of blood volume, osmolarity and blood pressure. Therefore, sodium plasma concentration is maintained within a relatively narrow range of around 140 mmol/L. The sodium concentration in the interstitial space can be though much higher though (Jantsch et al., 2015, Szabo and Magyar, 1982, Wiig et al., 2013). Animal studies suggest that dietary salt loading can result in hypertonic sodium storage in the skin by binding to glycosaminoglycans. Sodium clearance from the skin is mediated by mononuclear phagocyte system-derived VEGF-C-induced lymphangiogenesis (Machnik et al., 2010, Machnik et al., 2009). Blockade of lymph-endothelial VEGFC receptor VEGFR3 induced salt-sensitive hypertension, suggesting that skin sodium homeostasis is directly connected to blood pressure regulation (Wiig et al., 2013). Recent development of ^{23}Na-MRI enabled the non-invasive quantification and visualization of sodium in skin and soft tissues of humans non-invasively (Kopp et al., 2012). ^{23}Na-MRI studies demonstrated that hypertensive patients have a higher skin sodium content, thereby confirming findings of animal studies (Kopp et al., 2013). Additionally, skin sodium content was found to increase with ageing (Kopp et al., 2013) and in patients with reduced kidney function (Dahlmann et al., 2015, Kopp et al., 2018, Schneider et al., 2017).

In the skin microenvironment, higher sodium concentrations enhance macrophage function and might thus serve as a protective factor against microbial invaders (Jantsch et al., 2015). Furthermore, several groups provided strong evidence that an elevated sodium concentration has immunomodulating effect (Schatz et al., 2017, Wilck et al., 2019) by augmenting pro-inflammatory and antimicrobial macrophage function as well as T cell activation (Binger et al., 2015, Jantsch et al., 2015, Kleinewietfeld et al., 2013, Wu et al., 2013, Zhang et al., 2015). Moreover, antitumor immunity was found to be enhanced by sodium-mediated functional

modulation of myeloid-derived suppressor cells, as well (Willebrand et al., 2019). Most importantly, differentiation and IL-17A production of pathogenic interleukin (IL)-23-dependent Th17 cells could be boosted by elevated local sodium concentrations (Kleinewietfeld et al., 2013).

IL-17A is a central factor in the pathogenesis of psoriasis (Blauvelt, 2008, Kurschus and Moos, 2017, Schon and Erpenbeck, 2018). IL-17A produced by Th17 cells as well as γδ T cells of the skin (O'Brien and Born, 2015) evokes – in concert with other inflammatory cell types – an inflammatory circuit ultimately resulting in the classical clinical picture of psoriasis with hyper- and parakeratosis, erythema, scaling and neutrophil abscess formation (Lowes et al., 2013, Wagner et al., 2010). Indeed, inhibitors of this pathway were proved to be a highly effective treatment strategy (Nast et al., 2018, Reich et al., 2019, Tomalin et al., 2020, Waisman, 2012). Based on the recent findings on the interplay of IL-17A and sodium, we investigated the role of skin sodium in psoriasis by testing the hypotheses that skin sodium content and concentration is elevated 1) in psoriasis patients as well as 2) in murine psoriasis models, and 3) that skin sodium content reflects disease severity. We therefore initiated an observational study to measure skin sodium content as well as concentration by non-invasive MRI-based methods in patients with psoriasis vulgaris and in healthy control subjects. Direct electrolyte measurements of ashed-skin biopsies of psoriatic patients and healthy subjects by atomic adsorption spectrometry was applied to verify MRI findings. In parallel, we analysed skin sodium and potassium content in three translational mouse models of psoriasis-like skin disease. Finally, we investigated *in vitro* the Th17 differentiation modifying potential of a higher NaCl milieu of naïve $CD4^+$ cells of psoriatic patients. Our human and murine data suggest a disease severity-dependent and inflammation-associated, potentially disease modifying sodium accumulation in the skin and thus a yet unrecognized pathophysiological feature of psoriasis.

RESULTS

Sodium content in non-lesional skin of psoriasis patients correlates with disease severity and inflammation.

We screened 37 psoriasis patients and 19 controls of which 18 and 14 met criteria to enter our study for analysis of sodium content with ^{23}Na-MRI, respectively (Supplementary Figure S1). There were no significant differences in general patient characteristics of psoriasis patients and healthy control subjects (Supplementary Table 1). Due to the technical properties of the ^{23}Na knee-coil, skin sodium was measured on the flexor site of the calf, which usually shows no psoriatic lesions (as in all of our cases). Since psoriasis is a systemic disease and biochemical and structural changes can be detected in non-lesional skin too (Zurauskas et al., 2020), we hypothesized that we would be able to detect potential changes of skin sodium content in the non-lesional skin, as well. Skin sodium levels between psoriasis patients and control subjects were not significantly different (Supplementary Figure S2). However, stratifying psoriasis patients according to their disease severity, patients with moderate disease activity (defined as psoriasis area and severity index (PASI) > 5), separated clearly and significantly from those of with mild or no disease activity (PASI < 5) as well as from healthy controls (Figure 1a). In agreement, we found a significant, positive correlation between skin sodium content and PASI (Figure 1b). The increase in sodium content in patients with a PASI > 5 was paralleled by an increase in skin water content, which was measured simultaneously (Figure 1c). To determine if increased sodium content is a limited to the skin of psoriasis patients, we also investigated sodium content in the soleus muscle. We found that sodium levels in muscle neither differed between the groups (Figure 1d), nor correlated with PASI in psoriatic patients (Figure 1e). There was no difference in muscle water content either (Figure 1f). Representative ^{23}Na-MRI and ^{1}H images of age-matched healthy controls and psoriasis patients with mild (PASI = 3.1) and moderate (PASI = 6.9) disease activity are shown in Figure 1g. When comparing laboratory

parameters of psoriasis patients with PASI < 5 and healthy controls psoriasis patients with PASI > 5 had higher serum high-sensitivity C-reactive protein levels (hsCRP), serum lactate dehydrogenase (LDH) and aspartate transaminase (AST) levels (Table 1).

Next, we investigated whether skin sodium content correlates with counts and with specific subsets of blood leukocytes. Indeed, we found that skin sodium content of psoriasis patients correlated significantly and positively with leukocytes and neutrophil counts in peripheral blood as well as with hsCRP (Figure 2, a-c). Additionally, skin sodium content of patients showed positive correlation with serum urea concentrations (but not with serum creatinine or with estimated glomerular filtration rate), LDH and AST levels and with the BMI (Supplementary Figure S3, a-f).

Furthermore, we analyzed peripheral blood mononuclear cells (PBMC) of psoriasis patients by flow cytometry. To identify and quantify Th1, Th17 and circulating IL-17A$^+$ γδ T cells in psoriasis patients, intracellular cytokine expression for IL-17A and IFN-γ was assessed as well as surface marker γδ TCR of the respective CD4$^+$ and CD4$^-$ cell fractions. Th1 cells were defined as IFNγ$^+$IL17A$^-$ populations and Th17 cells as IL17A$^+$IFNγ$^-$ (Kagami et al., 2010). Whereas populations Th1 and Th17 cells did not correlate significantly (r=0.31, p=0.22 and r=0.4, p=0.11, respectively) circulating IL-17$^+$IFNγ$^-$ γδ TCR$^+$ cells correlated positively and significantly with skin sodium content (Figure 2, d and e).

To measure sodium concentrations, we applied ^{23}Na-spectroscopy in a subset of the patients who had ^{23}Na-MRI measurement, as well. This method has not only a significantly better resolution of the skin and therefore a much better sensitivity to measure skin sodium but also allows measurements on different body regions due to its flexible application. In this way, we were able to measure and compare non-lesional and lesional skin of the same patient, exemplifying the advantage of this technology. In Figure 3a and b, representative skin ^{23}Na-magnetic resonance spectrograms are shown of a patient with a PASI score of 9.6, depicting

internal standard sodium peak shifted by Tm (first peak) and skin sodium peak (second) of non-lesional and lesional skin as well as high resolution ^{1}H images of the same skin region, respectively. Lesional skin did not contain *per se* significantly higher skin sodium concentrations compared to non-lesional skin areas. (Figure 3c). Still, we could verify the findings gained by ^{23}Na-MRI knee-coil, namely that skin sodium concentration is significantly higher in psoriasis patients with PASI > 5 compared to those with PASI < 5 or healthy controls (Figure 3d). To further verify this finding, we measured *ex vivo* electrolyte and water content of lesional and non-lesional skin biopsies of psoriatic patients with PASI > 5 and of healthy control subjects by atomic adsorption spectrometry. These data showed elevated skin Na^+ content in ashed-skin biopsies of psoriatic patients. Nevertheless, we did not observe a difference between non-lesional and lesional skin biopsies (Supplementary Figure 4a). Similar observations were made for potassium and water content (Supplementary Figure 4b and c). More importantly, we measured significantly higher Na^+ plus K^+ concentrations in the lesional skin of psoriasis patients with PASI > 5 (Supplementary Figure 4d). These data confirmed the results we had measured by ^{23}Na-MRI and with ^{23}Na-spectroscopy.

Media with elevated sodium chloride concentrations promotes Th17-cell induction

To address possible effect of an altered electrolyte milieu on immune cells we differentiated naïve $CD4^+$ lymphocyte of psoriasis patient with either PASI < 5 or PASI > 5 into Th17 cells in the presence (NaCl) or absence (Iso) of an additional 40 mM NaCl in the differentiation culture media and analyzed the cells after differentiation by flow cytometry for IL-17A. Similar to earlier published data where $CD4^+$ lymphocyte of healthy subjects were investigated (Kleinewietfeld et al., 2013), we found that differentiated naïve $CD4^+$ lymphocyte of psoriasis patients, independent of disease activity, expressed significantly more IL-17A under higher NaCl concentrations as determined by flow cytometry (Figure 4a-c).

Murine imiquimod (IMQ)-induced psoriasis-like skin inflammation model recapitulates psoriasis patient findings and renders elevated water content of intracellular origin.

Skin sodium and water content were elevated in psoriasis patients with PASI > 5. To investigate whether elevated sodium content is associated with immune cell infiltration and hyperproliferation and to investigate the nature of elevated water content, we used the murine model of IMQ-induced skin inflammation. First, we characterized our model with regard to electrolyte and water content. Treatment of shaved dorsal skin and both ears of FVB/NCrl mice with the toll-like receptor 7 and 8 agonist IMQ over 6 days provoked an acute severe psoriasis-like skin phenotype (Figure 5a) including skin thickening, scaling of the skin and local erythema provoking elevated modified PASI scores and expression of IL-17A in the skin (Figure 5b and Supplementary Figure 5a-d) as previously described (Schuler et al., 2019, van der Fits et al., 2009). Skin alterations were accompanied by significantly elevated sodium content in both the lesional dorsal skin (application area of IMQ) and the non-lesional ventral skin (remote area without direct IMQ application) of IMQ-treated mice compared to sham treated mice (Figure 5c). Skin water content behaved similarly as skin sodium content (Figure 5d), concordant with our findings with human psoriasis patients.

In the mouse IMQ-induced psoriasis model we measured potassium as well as a surrogate marker for cell density. Skin potassium content was also increased in the IMQ application area, but not in the untreated remote skin area compared to sham treated mice (Figure 5e) suggesting an elevated cellular component per gram dry weight in the IMQ application area of the skin. Sham treated animals had similar sodium, water and potassium content and sodium plus potassium to total skin water ratio in both dorsal and ventral skin area (Figure 5, c-f). These electrolyte contents reflect a shift of the proportion of extra- and intracellular volumes. Nevertheless, sodium plus potassium to total skin water ratio was significantly higher in the

IMQ application area of the skin reflecting a clear electrolyte excess (Figure 5f). As water content was assessed by tissue drying, separate calculation of intra- and extracellular water content could not be performed. Thus, we next assessed the extracellular distribution volume of the tracer ^{51}Cr-EDTA in order to measure extracellular volumes of IMQ- and sham-treated mice. Interestingly, sham- and IMQ-treated skin (ear and dorsal skin) presented similar extracellular water volumes (Figure 5g). Additionally, dorsal skin samples were cut into 20 µm consecutive horizontal sections and ^{51}Cr-EDTA was counted in a gamma counter. Because of the epidermal hyperproliferation, IMQ-treated skin exhibited lower extracellular volumes until a depth of 40 µm (average thickness of dorsal epidermis of IMQ-treated mice was 28 µm (± SD of 8 µm) (Figure 5h). Below a cutting depth of 40 µm, representing dermis in both sham and IMQ-treated animals, extracellular volume was again similar (Figure 5g). This data suggests that capillary leakage in IMQ-induced psoriatic like skin alteration is compensated by cellular uptake of water or per se does not lead to considerable capillary leakage.

The imiquimod murine model has recently been critically evaluated and limitations have been identified (Hawkes et al., 2017). Therefore, we measured electrolyte and water content in an allergic contact-dermatitis model induced by 2,4,6 trinitrochlorobenzene (TNCB) (Esser and Martin, 2017) to control for epidermal edema or spongiosis. Mice were sensitized on the abdominal skin using TNCB or solvent only as vehicle and 5 days later, ears of the mice were challenged. One ear received TNCB and the other vehicle as an internal control for the challenge effect. TNCB treatment led to skin thickening (Supplementary Figure 6a). Similar to the IMQ model, we measured in sensitized animals with challenged ear skin elevated sodium, potassium, and water content, whereas skin sodium plus potassium concentration was not different in these animals compared to any of the experimental control groups (Supplementary Figure 6b-e). These findings suggest that in this allergic model, elevation in skin sodium and potassium content is followed by the respective water content elevation unlike in the IMQ

psoriasis mouse model. These data strongly argue for a specific electrolyte shift in the IMQ model for psoriasis.

Finally, we measured inflammatory immune cells in both the spleen and draining axillary and cervical lymph nodes by flow cytometry. Both spleen and draining lymph nodes of IMQ-treated mice showed elevated IL-17A-producing γδ TCR^+ cell frequencies (Supplementary Figure 7a-c), whereas IL-$22^-IFN\gamma^+$ $CD8^+$ and $CD4^+$ frequencies were only elevated in regional lymph nodes (Supplementary Figure 7d-i). Of the investigated lymphocyte populations, $IFN\gamma^+$IL-22^- $CD8^+$ and $CD4^+$ cells of draining lymph nodes (axillary and cervical) were significantly and positively correlated with skin sodium content (Figure 7i-l).

Skin sodium content of IL-17A-driven genetic psoriasis mouse models correlates with skin disease severity.

Based on the significantly altered dermal electrolyte composition in the short-term drug-induced psoriasis mouse model, we subsequently analysed how chronic IL17A-driven genetic murine psoriasis models – which better mimic the chronic nature of the human skin disease – impact on dermal electrolyte levels. Heterozygous CD11c-IL-$17A^{ind/+}$ mice and homozygous CD11c-IL-$17A^{ind/ind}$ mice express IL-17A in $CD11c^+$ dendritic cells and present a moderate to severe psoriasis-like skin phenotype with a more delayed onset (Wohn et al., 2016) compared to K14-IL-$17A^{ind/+}$ mice, which overexpress IL-17A in the K14 keratinocytes (Croxford et al., 2014). Kinetics of skin lesion development and disease severity was described to be IL-17A dose-dependent (Croxford et al., 2014, Schuler et al., 2019, Wohn et al., 2016). Representative images of the skin phenotype of the genetic psoriasis mouse models as well as histological staining of IL-17A of the ears are shown in Figure 6a reflecting the correlation between skin disease severity and skin IL-17A content. Skin thickening (measured as ear skin thickness) and modified PASI score of CD11c-IL-$17A^{ind/+}$, CD11c-IL-$17^{ind/ind}$ and K14-IL-$17A^{ind/+}$ mice

compared to IL-17A$^{ind/+}$ control mice are shown in Figure 6b and c. Consistent with our human findings and the findings in acute IMQ-induced psoriasis-like skin inflammation in mice, we found an elevated skin sodium content in all analysed genetic psoriasis models compared to healthy littermate controls (Figure 6d). Whereas all models also showed an elevated skin sodium content compared to healthy littermate controls (Figure 6d), skin water and potassium content was further, gradually to severity of the mouse model, increased (Figure 6, e and f). Sodium plus potassium to total skin water ratio was significantly higher in all genetic psoriasis mouse models (Figure 6g), similarly to the IMQ-induced psoriasis-like skin inflammation, reflecting again an excessive electrolyte accumulation in the skin. Skin sodium content correlated with skin disease severity in heterozygous CD11c-IL-17A$^{ind/+}$ and homozygous CD11c-IL-17A$^{ind/ind}$ mice (Figure 6h). Comparing all three chronic psoriasis models by using ear thickness as a proxy for disease severity as a valid, comparable and quantitative measure across all models, skin sodium content correlated directly with ear thickness and thus with skin disease severity across the models (Figure 6i).

DISCUSSION

Patients with psoriasis suffer from a dysregulated immune system. In the last decade, animal models of psoriasis helped to identify the interleukin IL-23/IL-17 axis as central in pathogenesis of psoriasis (El Malki et al., 2013, van der Fits et al., 2009). Whereas polymorphisms have been found in genes involved in IL-23 signaling and Th17 cell adaptive immune responses (Capon et al., 2012), there is strong evidence that non-genetical factors, such as elevated local sodium concentration can also boost the development of pathogenic IL-23-dependent Th17 cells (Kleinewietfeld et al., 2013). To test the hypothesis that psoriasis patients have elevated skin sodium content we measured skin sodium levels in psoriasis patients and age-matched healthy controls using non-invasive ^{23}Na-MRI methods (Jantsch et al., 2015, Kopp et al., 2012). We

found that disease severity, assessed by PASI, correlated significantly with skin sodium content. Similar observation was made by Kopp et al. systemic sclerosis patients (Kopp et al., 2017). The authors assessed the amount of sodium in the forearm skin using a similar ^{23}Na-MRI technique and found that sodium levels positively correlate with the degree of the disease activity assessed by the European Scleroderma Trials and Research Disease Activity Score (Kopp et al., 2017).

Additionally, Matthias et al. found that patients with atopic dermatitis, a type-2 immune disease, also present with elevated skin-sodium concentrations in their lesional skin, compared to non-lesional atopic and healthy skin (Matthias et al., 2019). They showed *in vitro* that sodium chloride potently promotes Th2 cell responses. We found that elevated sodium chloride concentration can boost Th17 differentiation of naïve $CD4^+$ cells of psoriatic patients. These data suggest that diseases with skin involvement of different immune-derivation types are associated with higher skin sodium concentration, which can potentially modify T-cell differentiation in an unfavorable manner. Further studies are needed to establish a causative link between skin-sodium accumulation and the regulation of immune-cell function.

Skin sodium content positively and significantly correlated with classical inflammatory markers like CRP and white blood cell count as well as with non-conventional inflammatory parameters like LDH and urea reflecting tissue damage and catabolic state, respectively. A recent study suggests that a high salt diet induces a catabolic state for urea osmolyte generation in order to conserve body water (Kitada et al., 2017). The elevated serum urea (independently from kidney function) and its association with elevated skin sodium content in psoriasis patients with active disease might indicate that similar biochemical processes are occurring in this patient group. Taken together, our findings argue strongly that skin sodium is associated with disease and inflammation severity.

Of special interest, flow cytometric analysis of peripheral blood cells identified circulating IL-17A-producing γδ T cells as correlates of skin sodium content. It has long been established that large numbers of IFNγ-producing $CD4^+$ T cells (Cai et al., 2012) circulate in the blood of psoriatic patients. IL-17A-secreting γδ T cells, on the contrary, have been described mainly in psoriatic skin lesions where they are considered to be the major IL-17 producers in the skin (Cai et al., 2011). Nevertheless, some studies suggest that IL-17-producing γδ T cells expand during autoimmune inflammation and infiltrate target tissues via circulation (McKenzie et al., 2017, Sutton et al., 2009). Detection of IL-17-secreting γδ T cells in the systemic circulation and its correlation with skin sodium content might suggest that these cells escape the skin in active psoriasis.

Skin sodium increase appeared to be water coupled in human psoriasis patients, and one could interpret this as a result of inflammation-caused increased vascular permeability, although none of the patients presented clinically apparent edema. Indeed, some studies suggest that psoriatic lesions – and even non-lesional skin of psoriatic patients – show vascular alterations such as angiogenesis, dilation of capillary beds, tortuosity of capillary loops and increased capillary permeability (Barton et al., 1992, Chua and Arbiser, 2009, Nickoloff, 2000). To address the extent of extracellular volume expansion, we turned to the mouse experimental approach of IMQ-induced psoriasis-like skin inflammation serving as acute severe psoriasis model. In line with the ^{23}Na-MRI measurements in human patients, we observed significantly elevated sodium content in the skin of IMQ-treated mice compared to sham-treated mice. Furthermore, skin potassium content was elevated in IMQ-treated dorsal skin area as well. As potassium mainly derives from intracellular space, we hypothesized that elevated skin potassium content corresponded to epidermal hyperplasia and influx of immune cells. An increase in cell numbers results in an increase of intracellular water content which ultimately should lead to increased total water, as we observed. In order to test the hypothesis that excessive water was of

intracellular origin rather than extracellular origin, we quantified the extracellular fluid volume in IMQ and sham-treated dorsal skin and ears of mice with the extracellular tracer ^{51}Cr-EDTA. Thereby, we could show that extracellular fluid volumes were similar in IMQ and sham-treated mice suggesting that possible increased vascular permeability and hyperfiltration does not lead directly to excessive extracellular volume expansion and ultimately to edema. Applying this finding to the results of the ^{23}Na-MRI measurements in psoriasis patients would mean elevated extracellular sodium concentrations in the skin, which could contribute to enhanced IL-17A production in the skin by influencing Th17 differentiation. The findings in our *in vitro* Th17 cell differentiation of naïve $CD4^+$ T cells from psoriatic patients under elevated sodium-chloride levels support that point of view. Nevertheless, a direct translation of findings from an animal model to human disease has its limitations and therefore this hypothesis must be addressed in further human studies. While our measurements do not allow deducing exact concentrations of electrolytes in the different tissue compartments with complete certainty, we measured higher total sodium plus potassium concentration in the skin of all psoriasis mouse models which unambiguously implies electrolyte accumulation in lesional skin.

In a sub-cohort of our human study, we measured and compared lesional and non-lesional sites of the leg of the same participant using ^{23}Na-spectroscopy, as well. Here, the sodium concentrations of lesional and non-lesional sites were not significantly different. This is in line with recent findings of Matthias et al. (Matthias et al., 2019) who measured sodium content by neutron activation analysis in lesional and non-lesional skin punch biopsies of psoriasis patients. It has to be considered that both approaches - the study of Matthias et al. and ours - investigated a very limited number of patients. As psoriasis patients with PASI >5 appear to have higher sodium concentrations in the lesional skin vs. non-lesional skin, we followed up this open question and performed direct skin electrolyte measurements on skin biopsies of psoriatic patients with PASI >5, as well as with skin biopsies from healthy controls. These data

showed elevated skin sodium levels in biopsies from psoriatic patients. Nevertheless, we again failed to observe a difference between non-lesional and lesional skin biopsies.

In line with our findings in IMQ-treated mice, the chronic IL17A-driven genetic psoriasis mouse models K14-IL-17A$^{ind/+}$ (severe chronic psoriasis based on overexpression of IL-17A locally in K14-positive keratinocytes) and CD11c-IL-17A$^{ind/+}$ (moderate to severe psoriasis based on overexpression of IL-17A in dendritic cells) also showed elevated skin sodium content. In these models, dermal and systemic IL-17A levels correlate with disease severity (Croxford et al., 2014, Schuler et al., 2019, Wohn et al., 2016). We used this fact to test the hypothesis that disease severity (and in this case higher cytokine levels and inflammation) leads to higher skin sodium levels. Indeed, similar to our human findings with different PASI scores, disease severity (quantitatively assessed by ear thickness measurement) correlated positively with skin sodium content in mice.

Our study has limitations. In our human study cohort, the number of patients with high PASI score was low and a few laboratory parameters differed from those psoriasis patients with PASI <5. Of note, we included patients with local treatment only (except treatment with dimethyl fumarate in patient with PASI > 5) in order to exclude the effect of systemic treatment on blood immune cells, further limiting our chances to recruit patients with high PASI scores. Nevertheless, we performed further electrolyte measurements with skin biopsies from additional psoriasis patients with PASI >5, as well as with skin biopsies of healthy control subjects using a method (atomic adsorption spectrometry) other than MRI. This direct measurement affirmed our findings with ^{23}Na-MRI and ^{23}Na-spectrometry. Moreover, early X-ray microanalysis of the skin layers also support our findings (Grundin et al., 1985). To keep the study more feasible for psoriasis patients and due to the doubts of the value of a single 24-hour urine collection as predictor for sodium intake we did not assess sodium consumption (Lerchl et al., 2015). Nevertheless, possible effects of dietary sodium as an environmental factor

on disease activity, skin sodium content and IL-17A-producing immune cells should be subject of further studies. Especially, as there are no clinical or experimental studies examining the relationship between salt consumption and psoriasis whereas data from animal models of multiple sclerosis, colitis and arthritis already indicated a link between increased IL-17 and dietary salt (Aguiar et al., 2017, Hernandez et al., 2015, Jung et al., 2019, Toussirot et al., 2018). Indeed, one important aspect of (severe) psoriasis is its association with hypertension and in general with cardiovascular comorbidity ((Mehta et al., 2010, Neimann et al., 2006, Takeshita et al., 2015). The association between psoriasis (or IL-17A driven autoimmune diseases in general), hypertension, and cardiovascular disease is of clinical relevance; however, up to now incompletely understood. The disturbances in local sodium homeostasis described herein could be a factor, especially since higher skin sodium concentrations were found in hypertensive patients (Kopp et al., 2013).

Taken together, our human data and findings of animal models argue for skin sodium accumulation in active psoriasis, which was elevated independently of extracellular volume as indicated by ^{51}Cr-EDTA measurements in the murine IMQ-induced psoriasis-like model. Skin sodium was strongly associated with the severity of skin inflammation in both humans and mice and associated with increased IL-17A-producing γδ T cells in peripheral blood in humans. Further studies are needed for a better understanding of the pathophysiology of the complex electrolyte changes of the psoriatic skin.

METHODS

See Supplementary Materials online for details.

Studies with psoriasis patients and healthy controls

The ethics committee of the Charité – Universitätsmedizin Berlin reviewed and approved this cross-sectional observational study (approval reference number: EA1325/13, ClinicalTrials.gov Identifier: NCT04095130). Skin biopsies were obtained from patients from another study with an approval reference number 2018-13105KliFo (Ethics Committee of the Medical Association of Rheinland-Pfalz). Clinical investigations have been conducted according to the principles of the Declaration of Helsinki. Written informed consent was received from all participants prior to inclusion in the study.

^{23}Na-MRI estimation of skin Na^+ content in humans

Measurements were done by previously validated methods (Kopp et al., 2012, Roth et al., 2019). Images obtained were analysed using ImageJ 1.50i software (NIH, USA) and the Tudor DICOM plugin as described in details earlier (Roth et al., 2019).

^{23}Na-spectroscopy of skin Na^+ content in humans

^{23}Na-spectroscopy measurements were performed as described earlier (Jantsch et al., 2015).

Mouse models of psoriatic skin disease

Crossing of the IL-17A$^{ind/ind}$ mouse strain with K14-Cre or CD11c-Cre resulted in K14-IL-17A$^{ind/+}$ (Croxford et al., 2014), CD11c-IL-17A$^{ind/+}$ or CD11c-IL-17A$^{ind/ind}$ mice (Wohn et al., 2016). Apart from the genetic models, psoriasis-like skin disease was drug-induced by topical dose of 62.5 mg of commercially available IMQ cream (5%) (Aldara; 3M Pharmaceuticals) on the shaved back and on both ears for 6 consecutive days, on 12-week-old FVB/NCrl (Charles River, Germany) mice, as described earlier (El Malki et al., 2013, van der Fits et al., 2009). Sham animals underwent the same procedure except creaming with IMQ. All animals were housed and treated in accordance with Directive 2010/63/EU of the European Parliament on

the protection of animals used for scientific purposes and institutional guidelines of the Translational Animal Research Center of the University Medical Center Mainz, Germany and Animal Facility of the Max Delbrück Center for Molecular Medicine in the Helmholtz Association Berlin, Germany. Mice were held in specific pathogen free (SPF) condition, 12:12 h day:night cycle, and with free access to purified food (E15430-047, Ssniff, Soest, Germany) and water. Experiments were approved by the Animal Care and Use Committee from the Land of Rhineland-Palatine, approval numbers G13-1-099 and G15-1-051 and by the Berlin Animal Review Board, Berlin, Germany (IMQ studies; G090/13).

PASI scoring in mouse models

We determined the severity of psoriasis-like skin disease by modified PASI scoring, as described previously (El Malki et al., 2013, Karbach et al., 2014).

2,4,6 trinitrochlorobenzene (TNCB)-induced allergic contact dermatitis model

Male, 16 week-old, Ly5.1/Ly5.2 mice on C57BL/6 background were bred in the animal facility of the Interfacultary Biomedical Faculty in Heidelberg, Germany, under specified pathogen-free (SPF) conditions. The animal studies were performed with approval from the respective authorities (Kurschus, 35-9185.81/G-1/19) and were conducted by certified personnel.

At day 0, the abdomen of mice was shaved manually using a trimmer. Then, mice were sensitized either with 15 µl of 1% TNCB dissolved in 4/5 acetone and 1/5 miglyol (Vehicle) or with Vehicle only on the shaved abdomen applied by a pipette. The role of acetone is to extract lipids from the outer layer of the stratum corneum, disrupting the epidermal barrier and ensure an efficient antigen administration. At day 5, mice were challenged on the right ear by applying a total volume of 20 µl of 0.5% TNCB dissolved in 4/5 acetone and 1/5 miglyol (Vehicle) both sides (10 µl each) of the ear. As a control, the left ear was treated with Vehicle only. Ear

swelling reaction was measured 6, 24 and 48 h after challenge.

Flow cytometric analysis

Human PBMC and immune cells of mice were processed and analysed as described previously (Mahler et al., 2018, Wilck et al., 2017) and as described in the online supplementary material.

Measurement of electrolyte and water content in human skin biopsies and in the mouse skin

Electrolyte measurement was performed as described earlier (Machnik et al., 2009).

Statistical analysis

Statistical analysis was performed with GraphPad Prism 7 for Windows (GraphPad Software, La Jolla, CA) as described in the supplementary material. Data are presented as scatter dot plots with the mean±SD, where each individual represented by a single dot. Statistical significance is indicated as $*P \leq 0.05$, $**P \leq 0.01$, $***P \leq 0.001$.

Data availability statement. All data generated or analyzed during this study are included in this published article (and its supplementary information files).

Conflict of interest statement. The authors state no conflict of interest.

Acknowledgements. We thank Prof. Jens Titze (Duke-NUS Medical School, Singapore) for the helpful suggestions with the manuscript. We thank Dr. Leslie van der Fits for answering critical questions concerning the IMQ mouse model. We thank B. Schnackenburg and C. Stehning for the technical support with the MRI. We thank Dr. Kerstin Lommel, Maika Pluskat,

Dr. Sandra Burger and Dr. Magdalena Erdmann-Keding for their support with the patient recruitment. We thank G. N'diaye, M.-B. Köhler, I. Kamer, A. Schiche, N. Krüger, F. Bartelt, K. Perius, B. Kalt and A. Nikolaev for excellent technical support and T. Knopp for experimental help and advice. This work was partially funded by DFG grants KA 4035/1-1 (to SK) and by the Boehringer Ingelheim Foundation's "Novel and Neglected Cardiovascular Risk Factors: Molecular Mechanisms and Therapeutic Implications" and by the German Center of Cardiovascular Research (Deutsches Zentrum für Herz-Kreislauf- Forschung, DZHK) "Platelet Signatures and Psoriasis in Cardiac Dysfunction" (to SK and DNM). JW and SK were supported by the Federal Ministry of Education and Research (BMBF 01EO1503) related to this study. SK, BEC, AW and FCK were supported by the CRC/Transregio 156 ("The Skin as Sensor and Effector Organ Orchestrating Local and Systemic Immune Responses"). FCK was further supported by a DFG grant #444609457. JW is supported by the German Federal Ministry for Education and Research (BMBF EDU-V24) and the University of Mainz ('Inneruniversitäre Forschungsförderung'). HW was funded by grants from The Research Council of Norway (grant #262079) and The Western Norway Regional Health Authority (#303611). MK is a participant in the Charité Digital Clinician Scientist Program funded by DFG. NW is supported by the European Research Council (ERC) under the European Union's Horizon 2020 research and innovation program (852796) and by a grant from the Corona-Stiftung (Deutscher Stifterverband). NW is a participant in the Clinician Scientist Program funded by the Berlin Institute of Health (BIH). MKl was supported by the European Research Council (ERC) under the European Union's Horizon 2020 research and innovation program (640116), by a SALK-grant from the Government of Flanders and by an Odysseus-grant of the Research Foundation Flanders, Belgium (FWO).

Author contributions statement: DNM, SK and LM conceived the study. AM, JW, TVK, NR, EW, PL, VAGR, NW, FCK, and LM performed experiments., ABa, JW, TVK, NR, EW, PL, ABi, TB and LM analyzed the data. JW and LM prepared the figures. JW, AM and LM performed statistics. MB, FCL and DNM wrote the clinical study proposal. AK, GK, and SP coordinated patient recruitment. LM recruited patients with the help of GK, JWe and MS. RD, FCL, MKl, BEC, AW, HW and AB provided key technical and scientific support. MKe and TK provided MRI access and technical support together with PL. SK and LM wrote the manuscript with the input of all authors. LM coordinated the study. All authors reviewed and approved the manuscript.

TABLES

Table 1. Clinical characteristics of healthy subjects and psoriasis patients stratified by disease activity.

		Healthy subjects (n=12)		Psoriasis patient PASI<5 (n=13)		Psoriasis patient PASI>5 (n=5)		
Parameter	**Unit**	**Mean**	**SD**	**Mean**	**SD**	**Mean**	**SD**	**P-value**
Age	years	39.7	14.3	35.5	12.0	43.0	17.7	0.74
Gender	% male	50	n.a.	46	n.a.	100	n.a.	0.11
Smoker	% yes	25	n.a.	23	n.a.	40	n.a.	0.76
BMI	kg/m2	23.9	3.7	23.6	2.3	28.8	6.0	0.05
Sys BP	mmHg	120.7	10.2	118.1	11.5	120.2	12.3	0.85
Dias BP	mmHg	77.4	8.7	76.4	8.8	76.6	6.3	0.96
HR	beats/min	65.1	6.6	66.6	5.1	70.2	10.8	0.43
PVR	s*mmHg/mL	1.2	0.1	1.2	0.2	1.2	0.1	0.82
PWV	m/s	6.5	1.6	5.9	1.4	6.3	1.7	0.65
GGT	U/L	22.1	11.3	21.2	14.5	40.4	26.8	0.10
AST	U/L	23.1	4.1	21.7	4.5	34.4*	14.7	**0.01**
ALT	U/L	19.6	7.8	20.9	10.3	50.0*	49.9	0.05
LDH	U/L	173.3	22.2	163.5	25.1	208.6*	21.7	**0.01**
Creatinine	mg/dL	0.9	0.1	0.9	0.1	0.9	0.1	0.59
BUN	mg/dL	30.8	8.1	27.4	4.2	31.7	5.0	0.31
GFR	ml/min/1.73m^2	94.3	10.9	100.3	8.8	99.1	17.8	0.46
Sodium	mmol/L	141.3	1.5	141.9	2.2	142.4	2.2	0.59
Potassium	mmol/L	4.5	0.4	4.4	0.4	4.2	0.3	0.60

Chloride	mmol/L	100.9	1.8	100.5	1.9	101.2	2.3	0.80
Calcium	mmol/L	2.4	0.1	2.4	0.1	2.4	0.1	0.25
Hemoglobin	g/dL	13.9	1.0	14.4	1.2	14.4	0.6	0.39
Leukocytes	G/L	6.6	2.2	5.4	1.0	7.2	1.2	0.09
Neutrophils	G/L	4.2	2.0	2.8	0.9	4.5	1.2	0.06
Thrombocytes	G/L	250.8	52.5	211.5	36.7	239.6	64.3	0.17
hsCRP	mg/L	0.9	1.1	0.6	0.4	2.6*	2.3	**0.01**
HbA1c	%	5.3	0.3	5.3	0.2	5.4	0.1	0.61
TSH	mU/L	1.9	0.6	1.8	0.7	2.1	0.4	0.61

BMI, body mass index; BP, blood pressure; HR, heart rate; PVR, peripheral vascular resistance; PWV, pulse wave velocity; GGT, gamma-glutamyltransferase; AST, aspartate transaminase; ALT, alanine transaminase; LDH, lactate dehydrogenase; BUN, blood urea nitrogen; GFR, glomerular filtration rate; hsCRP, high sensitivity C-reactive protein; HbA1c, hemoglobin A1c; TSH, thyroid-stimulating hormone. *$p < 0.05$; n.a., not applicable.

FIGURE LEGENDS

Figure 1. Skin and muscle sodium and water content in healthy control and psoriasis patients measured by ^{23}Na-MRI. (a) Relative Na^+ intensity in the skin of healthy controls and in patients with PASI score below and above 5. (b) Correlation between relative Na^+ intensity in the skin and PASI score. (c) Relative water signal intensity in the skin controls and patient groups. (d) Relative Na^+ intensity in the muscle of healthy controls and in patients with PASI score below and above 5. (e) Correlation between relative Na^+ intensity in the muscle and PASI score. (f) Relative water signal intensity in the muscle in controls and patient groups. (g) Representative ^{23}Na-MRI (echo time (TE)=2.07 ms) images of the lower leg of a healthy control subject and of psoriasis patients with low PASI and high PASI score (upper panel). Representative water (^{1}H-MRI) images of the of the same subjects (lower panel). Tubes with solutions containing 10, 20, 30, and 40 mmol/L of NaCl are arranged below the extremity, thereby allowing us to calibrate tissue Na^+. ***P < 0.001; ns, not significant.

Figure 2. Skin sodium content of psoriasis patients measured by ^{23}Na-MRI correlates with inflammatory parameters and circulating IL-17$^+$ γδ T cells. Relative Na^+ intensity in the skin of psoriasis patients significantly and positively correlated with blood (a) total leukocyte count, (b) neutrophils and (c) high-sensitivity C reactive protein (hsCRP) concentrations. (d) Representative dot plot analyses of IL17A and IFNγ expression in circulating stimulated $CD3^+CD4^-\gamma\delta TCR^+$ cells (after live-dead and doublet exclusion) of psoriasis patients. IL-$17^+IFN\gamma^-\gamma\delta TCR^+$ cells correlate significantly and positively with relative skin Na^+ intensity of psoriasis patients.

Figure 3. Skin sodium concentration in healthy control and psoriasis patients measured by ^{23}Na magnetic resonance spectroscopy. (a) Representative skin ^{23}Na magnetic resonance spectrogram of healthy (non-lesional, upper image) and psoriatic skin (lesional, lower image) of the same psoriatic patient. First peak is control peak (Na signal of 100 mmol/L Na^+ standard with shift reagent), second peak is Na^+ signal of the measured area. (b) High-resolution ^{1}H images for determination of skin thickness (white bars mark skin thickness). (c) Skin Na^+ concentrations measured by ^{23}Na magnetic resonance spectroscopy in healthy subjects (single dots) and in non-lesional and lesional skin of the psoriasis patients (dotted line connects measured concentrations in different skin regions of the same patients). (d) Skin Na^+ concentrations measured by ^{23}Na magnetic resonance spectroscopy of healthy controls and in patients with PASI score below and above 5. *P<0.05; **P < 0.01; ns, non-significant.

Figure 4. Salt enhances the Th17 polarization of naïve $CD4^+$ T cells of psoriasis patients *in vitro*. (a, b) Untouched naïve $CD4^+$ enriched T cell fractions of psoriatic patients were Th17-polarized *in vitro* under isotonic conditions or in the presence of additional 40 mM NaCl (NaCl) or absence (Iso). (a) and (b) denote representative flow cytometric plots of IL-17A and TNFα expression from psoriasis patient with (a) PASI < 5 and (b) PASI > 5 after *in vitro* Th17 polarization for seven days. (c) Quantification of the IL-17A and TNFα expressing cells after the in vitro polarization assay in presence (NaCl) or absence (Iso) of additional 40mM NaCl in the differentiation culture media. *P<0.05 for NaCl effect.

Figure 5. Skin sodium content is elevated in imiquimod (IMQ)-induced psoriasis-like skin disease and correlates with local inflammation. (a) Representative images of an IMQ-treated mouse and study design. (b) PASI score after 6 days of sham or IMQ treatment. (c) Sodium, (d) water (e) potassium content and (f) sodium plus potassium to water ratio of the dorsal

(application area) and ventral (remote area) skin of sham and IMQ-treated mice. (g) Extracellular volumes of sham and IMQ-treated mice in the application areas (ear and dorsal skin). (h) Extracellular volumes of sham and IMQ-treated mice in different depths of dorsal skin. (i) Correlation between IL-22$^-$IFNγ$^+$ CD8$^+$ and (j) IL-22$^-$IFNγ$^+$ CD4$^+$ cells of draining axillary lymph nodes with skin sodium content. (k) Correlation of IL-22$^-$IFNγ$^+$ CD8$^+$ and (l) IL-22$^-$IFNγ$^+$ CD4$^+$ cells of draining cervical lymph nodes with skin sodium content. **P < 0.01; ***P < 0.001; ns, non-significant.

Figure 6. Genetic overexpression of IL-17A in K14 or CD11c-positive cells leads to psoriasis-like skin disease and sodium accumulation in the skin. (a) Representative images and immunofluorescence-stained ear sections from healthy IL-17A$^{ind/+}$ control as well as from CD11c-IL-17A$^{ind/+}$ and K14-IL-17A$^{ind/+}$ mice (red: CD45.2; green: IL-17A; blue: DAPI). Scale bars equal 100 μm. (b) Ear thickness and (c) PASI scores of IL-17A$^{ind/+}$, CD11c-IL-17A$^{ind/+}$, CD11c-IL-17A$^{ind/ind}$ and K14-IL-17A$^{ind/+}$ mice. (d) Sodium, (e) water (f) potassium content and (g) sodium plus potassium to water ratio of the skin of IL-17A$^{ind/+}$, CD11c-IL-17A$^{ind/+}$, CD11c-IL-17A$^{ind/ind}$ and K14-IL-17A$^{ind/+}$ mice. (H) Correlation between relative skin Na$^+$ content and PASI score of CD11c-IL-17A$^{ind/+}$ and CD11c-IL-17A$^{ind/ind}$ mice. (i) Correlation between relative skin Na$^+$ content and ear thickness of IL-17A$^{ind/+}$, CD11c-IL-17A$^{ind/+}$, CD11c-IL-17A$^{ind/ind}$ and K14-IL-17A$^{ind/+}$ mice. *P < 0.05; **P < 0.01; ***P < 0.001; ns, non-significant.

REFERENCES

Aguiar SLF, Miranda MCG, Guimaraes MAF, Santiago HC, Queiroz CP, Cunha PDS, et al. High-Salt Diet Induces IL-17-Dependent Gut Inflammation and Exacerbates Colitis in Mice. Frontiers in immunology 2017;8:1969.

Barton SP, Abdullah MS, Marks R. Quantification of microvascular changes in the skin in patients with psoriasis. The British journal of dermatology 1992;126(6):569-74.

Binger KJ, Gebhardt M, Heinig M, Rintisch C, Schroeder A, Neuhofer W, et al. High salt reduces the activation of IL-4- and IL-13-stimulated macrophages. The Journal of clinical investigation 2015;125(11):4223-38.

Blauvelt A. T-helper 17 cells in psoriatic plaques and additional genetic links between IL-23 and psoriasis. The Journal of investigative dermatology 2008;128(5):1064-7.

Cai Y, Fleming C, Yan J. New insights of T cells in the pathogenesis of psoriasis. Cellular & molecular immunology 2012;9(4):302-9.

Cai Y, Shen X, Ding C, Qi C, Li K, Li X, et al. Pivotal role of dermal IL-17-producing gammadelta T cells in skin inflammation. Immunity 2011;35(4):596-610.

Capon F, Burden AD, Trembath RC, Barker JN. Psoriasis and other complex trait dermatoses: from Loci to functional pathways. The Journal of investigative dermatology 2012;132(3 Pt 2):915-22.

Chua RA, Arbiser JL. The role of angiogenesis in the pathogenesis of psoriasis. Autoimmunity 2009;42(7):574-9.

Croxford AL, Karbach S, Kurschus FC, Wortge S, Nikolaev A, Yogev N, et al. IL-6 regulates neutrophil microabscess formation in IL-17A-driven psoriasiform lesions. The Journal of investigative dermatology 2014;134(3):728-35.

Dahlmann A, Dorfelt K, Eicher F, Linz P, Kopp C, Mossinger I, et al. Magnetic resonance-determined sodium removal from tissue stores in hemodialysis patients. Kidney international 2015;87(2):434-41.

El Malki K, Karbach SH, Huppert J, Zayoud M, Reissig S, Schuler R, et al. An alternative pathway of imiquimod-induced psoriasis-like skin inflammation in the absence of interleukin-17 receptor a signaling. The Journal of investigative dermatology 2013;133(2):441-51.

Esser PR, Martin SF. Pathomechanisms of Contact Sensitization. Current allergy and asthma reports 2017;17(12):83.

Grundin TG, Roomans GM, Forslind B, Lindberg M, Werner Y. X-ray microanalysis of psoriatic skin. The Journal of investigative dermatology 1985;85(4):378-80.

Hawkes JE, Gudjonsson JE, Ward NL. The Snowballing Literature on Imiquimod-Induced Skin Inflammation in Mice: A Critical Appraisal. The Journal of investigative dermatology 2017;137(3):546-9.

Hernandez AL, Kitz A, Wu C, Lowther DE, Rodriguez DM, Vudattu N, et al. Sodium chloride inhibits the suppressive function of FOXP3+ regulatory T cells. The Journal of clinical investigation 2015;125(11):4212-22.

Jantsch J, Schatz V, Friedrich D, Schroder A, Kopp C, Siegert I, et al. Cutaneous Na+ storage strengthens the antimicrobial barrier function of the skin and boosts macrophage-driven host defense. Cell metabolism 2015;21(3):493-501.

Jung SM, Kim Y, Kim J, Jung H, Yi H, Rim YA, et al. Sodium Chloride Aggravates Arthritis via Th17 Polarization. Yonsei medical journal 2019;60(1):88-97.

Kagami S, Rizzo HL, Lee JJ, Koguchi Y, Blauvelt A. Circulating Th17, Th22, and Th1 cells are increased in psoriasis. The Journal of investigative dermatology 2010;130(5):1373-83.

Karbach S, Croxford AL, Oelze M, Schuler R, Minwegen D, Wegner J, et al. Interleukin 17 drives vascular inflammation, endothelial dysfunction, and arterial hypertension in psoriasis-like skin disease. Arteriosclerosis, thrombosis, and vascular biology 2014;34(12):2658-68.

Kitada K, Daub S, Zhang Y, Klein JD, Nakano D, Pedchenko T, et al. High salt intake reprioritizes osmolyte and energy metabolism for body fluid conservation. The Journal of clinical investigation 2017;127(5):1944-59.

Kleinewietfeld M, Manzel A, Titze J, Kvakan H, Yosef N, Linker RA, et al. Sodium chloride drives autoimmune disease by the induction of pathogenic TH17 cells. Nature 2013;496(7446):518-22.

Kopp C, Beyer C, Linz P, Dahlmann A, Hammon M, Jantsch J, et al. Na+ deposition in the fibrotic skin of systemic sclerosis patients detected by 23Na-magnetic resonance imaging. Rheumatology 2017;56(4):556-60.

Kopp C, Linz P, Dahlmann A, Hammon M, Jantsch J, Muller DN, et al. 23Na magnetic resonance imaging-determined tissue sodium in healthy subjects and hypertensive patients. Hypertension 2013;61(3):635-40.

Kopp C, Linz P, Maier C, Wabel P, Hammon M, Nagel AM, et al. Elevated tissue sodium deposition in patients with type 2 diabetes on hemodialysis detected by (23)Na magnetic resonance imaging. Kidney international 2018;93(5):1191-7.

Kopp C, Linz P, Wachsmuth L, Dahlmann A, Horbach T, Schofl C, et al. (23)Na magnetic resonance imaging of tissue sodium. Hypertension 2012;59(1):167-72.

Kurschus FC, Moos S. IL-17 for therapy. Journal of dermatological science 2017;87(3):221-7.

Lerchl K, Rakova N, Dahlmann A, Rauh M, Goller U, Basner M, et al. Agreement between 24-hour salt ingestion and sodium excretion in a controlled environment. Hypertension 2015;66(4):850-7.

Lowes MA, Russell CB, Martin DA, Towne JE, Krueger JG. The IL-23/T17 pathogenic axis in psoriasis is amplified by keratinocyte responses. Trends in immunology 2013;34(4):174-81.

Machnik A, Dahlmann A, Kopp C, Goss J, Wagner H, van Rooijen N, et al. Mononuclear phagocyte system depletion blocks interstitial tonicity-responsive enhancer binding protein/vascular endothelial growth factor C expression and induces salt-sensitive hypertension in rats. Hypertension 2010;55(3):755-61.

Machnik A, Neuhofer W, Jantsch J, Dahlmann A, Tammela T, Machura K, et al. Macrophages regulate salt-dependent volume and blood pressure by a vascular endothelial growth factor-C-dependent buffering mechanism. Nature medicine 2009;15(5):545-52.

Mahler A, Balogh A, Csizmadia I, Klug L, Kleinewietfeld M, Steiniger J, et al. Metabolic, Mental and Immunological Effects of Normoxic and Hypoxic Training in Multiple Sclerosis Patients: A Pilot Study. Frontiers in immunology 2018;9:2819.

Matthias J, Maul J, Noster R, Meinl H, Chao YY, Gerstenberg H, et al. Sodium chloride is an ionic checkpoint for human TH2 cells and shapes the atopic skin microenvironment. Science translational medicine 2019;11(480).

McKenzie DR, Kara EE, Bastow CR, Tyllis TS, Fenix KA, Gregor CE, et al. IL-17-producing gammadelta T cells switch migratory patterns between resting and activated states. Nature communications 2017;8:15632.

Mehta NN, Azfar RS, Shin DB, Neimann AL, Troxel AB, Gelfand JM. Patients with severe psoriasis are at increased risk of cardiovascular mortality: cohort study using the General Practice Research Database. European heart journal 2010;31(8):1000-6.

Nast A, Amelunxen L, Augustin M, Boehncke WH, Dressler C, Gaskins M, et al. S3 Guideline for the treatment of psoriasis vulgaris, update - Short version part 1 - Systemic treatment. Journal der Deutschen Dermatologischen Gesellschaft = Journal of the German Society of Dermatology : JDDG 2018;16(5):645-69.

Neimann AL, Shin DB, Wang X, Margolis DJ, Troxel AB, Gelfand JM. Prevalence of cardiovascular risk factors in patients with psoriasis. Journal of the American Academy of Dermatology 2006;55(5):829-35.

Nickoloff BJ. Characterization of lymphocyte-dependent angiogenesis using a SCID mouse: human skin model of psoriasis. The journal of investigative dermatology Symposium proceedings 2000;5(1):67-73.

O'Brien RL, Born WK. Dermal gammadelta T cells--What have we learned? Cellular immunology 2015;296(1):62-9.

Reich K, Armstrong AW, Langley RG, Flavin S, Randazzo B, Li S, et al. Guselkumab versus secukinumab for the treatment of moderate-to-severe psoriasis (ECLIPSE): results from a phase 3, randomised controlled trial. Lancet 2019;394(10201):831-9.

Roth S, Marko L, Birukov A, Hennemuth A, Kuhnen P, Jones A, et al. Tissue Sodium Content and Arterial Hypertension in Obese Adolescents. Journal of clinical medicine 2019;8(12).

Schatz V, Neubert P, Schroder A, Binger K, Gebhard M, Muller DN, et al. Elementary immunology: Na(+) as a regulator of immunity. Pediatric nephrology 2017;32(2):201-10.

Schneider MP, Raff U, Kopp C, Scheppach JB, Toncar S, Wanner C, et al. Skin Sodium Concentration Correlates with Left Ventricular Hypertrophy in CKD. Journal of the American Society of Nephrology : JASN 2017;28(6):1867-76.

Schon MP, Erpenbeck L. The Interleukin-23/Interleukin-17 Axis Links Adaptive and Innate Immunity in Psoriasis. Frontiers in immunology 2018;9:1323.

Schuler R, Brand A, Klebow S, Wild J, Veras FP, Ullmann E, et al. Antagonization of IL-17A Attenuates Skin Inflammation and Vascular Dysfunction in Mouse Models of Psoriasis. The Journal of investigative dermatology 2019;139(3):638-47.

Sutton CE, Lalor SJ, Sweeney CM, Brereton CF, Lavelle EC, Mills KH. Interleukin-1 and IL-23 induce innate IL-17 production from gammadelta T cells, amplifying Th17 responses and autoimmunity. Immunity 2009;31(2):331-41.

Szabo G, Magyar Z. Electrolyte concentrations in subcutaneous tissue fluid and lymph. Lymphology 1982;15(4):174-7.

Takeshita J, Wang S, Shin DB, Mehta NN, Kimmel SE, Margolis DJ, et al. Effect of psoriasis severity on hypertension control: a population-based study in the United Kingdom. JAMA dermatology 2015;151(2):161-9.

Tomalin LE, Russell CB, Garcet S, Ewald DA, Klekotka P, Nirula A, et al. Short-term transcriptional response to IL-17 receptor-A antagonism in the treatment of psoriasis. The Journal of allergy and clinical immunology 2020;145(3):922-32.

Toussirot E, Bereau M, Vauchy C, Saas P. Could Sodium Chloride be an Environmental Trigger for Immune-Mediated Diseases? An Overview of the Experimental and Clinical Evidence. Frontiers in physiology 2018;9:440.

van der Fits L, Mourits S, Voerman JS, Kant M, Boon L, Laman JD, et al. Imiquimod-induced psoriasis-like skin inflammation in mice is mediated via the IL-23/IL-17 axis. Journal of immunology 2009;182(9):5836-45.

Wagner EF, Schonthaler HB, Guinea-Viniegra J, Tschachler E. Psoriasis: what we have learned from mouse models. Nature reviews Rheumatology 2010;6(12):704-14.

Waisman A. To be 17 again--anti-interleukin-17 treatment for psoriasis. The New England journal of medicine 2012;366(13):1251-2.
Wiig H, Schroder A, Neuhofer W, Jantsch J, Kopp C, Karlsen TV, et al. Immune cells control skin lymphatic electrolyte homeostasis and blood pressure. The Journal of clinical investigation 2013;123(7):2803-15.
Wilck N, Balogh A, Marko L, Bartolomaeus H, Muller DN. The role of sodium in modulating immune cell function. Nature reviews Nephrology 2019;15(9):546-58.
Wilck N, Matus MG, Kearney SM, Olesen SW, Forslund K, Bartolomaeus H, et al. Salt-responsive gut commensal modulates TH17 axis and disease. Nature 2017;551(7682):585-9.
Willebrand R, Hamad I, Van Zeebroeck L, Kiss M, Bruderek K, Geuzens A, et al. High Salt Inhibits Tumor Growth by Enhancing Anti-tumor Immunity. Frontiers in immunology 2019;10:1141.
Wohn C, Brand A, van Ettinger K, Brouwers-Haspels I, Waisman A, Laman JD, et al. Gradual development of psoriatic skin lesions by constitutive low-level expression of IL-17A. Cellular immunology 2016;308:57-65.
Wu C, Yosef N, Thalhamer T, Zhu C, Xiao S, Kishi Y, et al. Induction of pathogenic TH17 cells by inducible salt-sensing kinase SGK1. Nature 2013;496(7446):513-7.
Zhang WC, Zheng XJ, Du LJ, Sun JY, Shen ZX, Shi C, et al. High salt primes a specific activation state of macrophages, M(Na). Cell research 2015;25(8):893-910.
Zurauskas M, Barkalifa R, Alex A, Marjanovic M, Spillman DR, Jr., Mukherjee P, et al. Assessing the severity of psoriasis through multivariate analysis of optical images from non-lesional skin. Scientific reports 2020;10(1):9154.

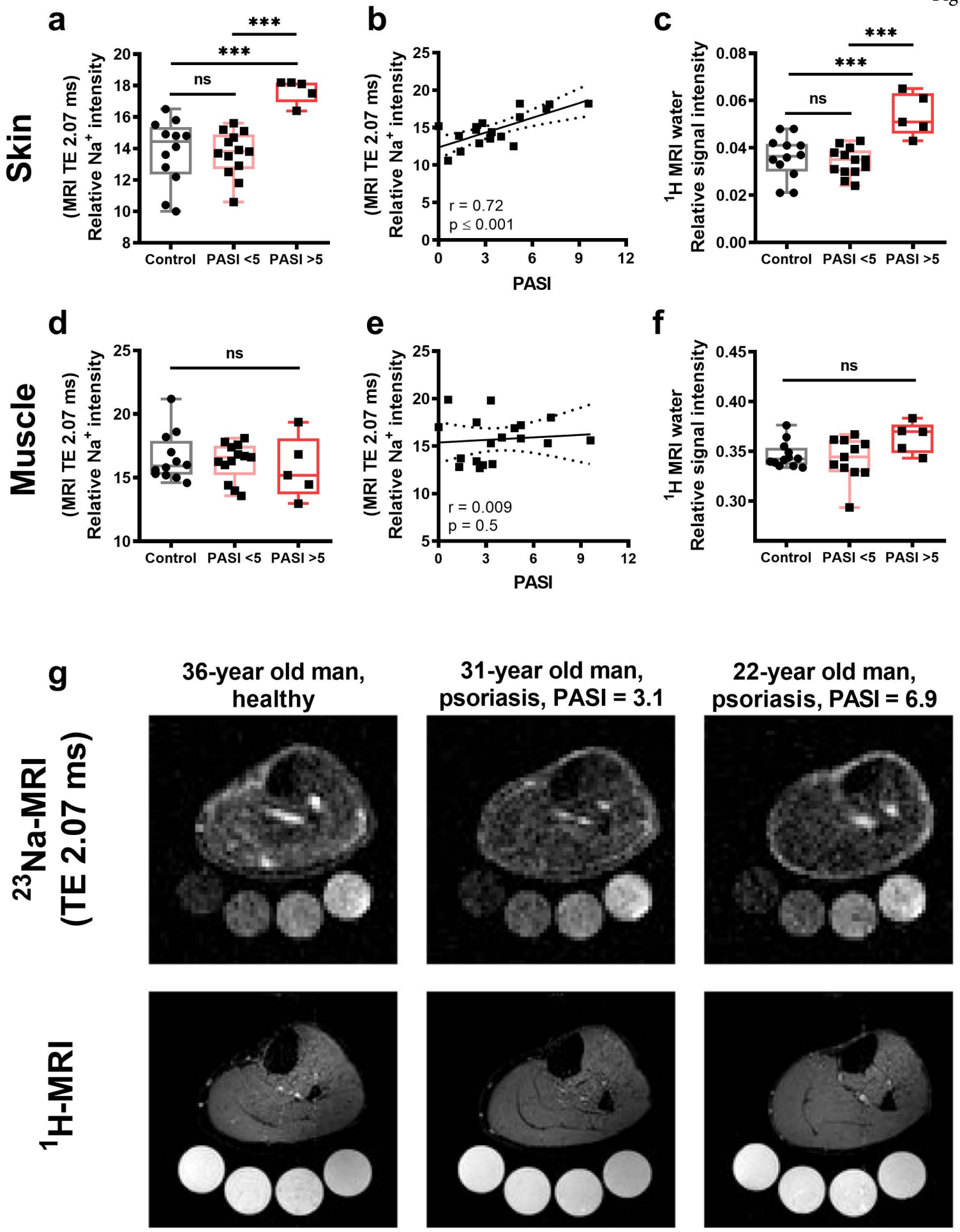
a
b
c
Skin
***
***
ns
(MRI TE 2.07 ms) Relative Na+ intensity
Control
PASI <5
PASI >5
r = 0.72
p ≤ 0.001
PASI
1H MRI water Relative signal intensity
d
e
f
Muscle
r = 0.009
p = 0.5
g
36-year old man, healthy
31-year old man, psoriasis, PASI = 3.1
22-year old man, psoriasis, PASI = 6.9
23Na-MRI (TE 2.07 ms)
1H-MRI

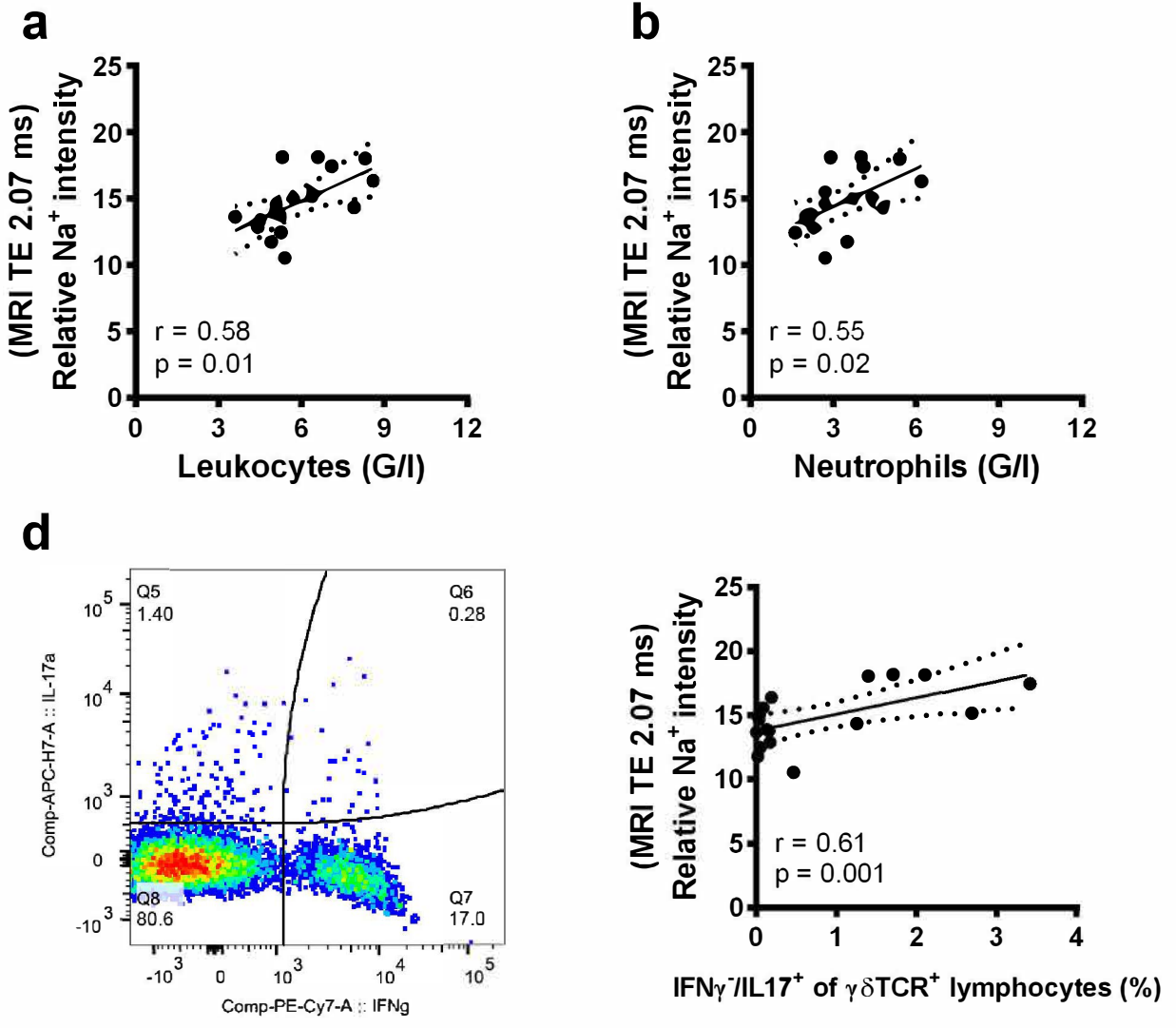
a
(MRI TE 2.07 ms) Relative Na+ intensity
Leukocytes (G/l)
r = 0.58
p = 0.01
b
(MRI TE 2.07 ms) Relative Na+ intensity
Neutrophils (G/l)
r = 0.55
p = 0.02
c
(MRI TE 2.07 ms) Relative Na+ intensity
hsCRP (mg/l)
r = 0.55
p = 0.02
d
Q5 1.40
Q6 0.28
Q8 80.6
Q7 17.0
Comp-APC-H7-A :: IL-17a
Comp-PE-Cy7-A :: IFNg
(MRI TE 2.07 ms) Relative Na+ intensity
IFNγ-/IL17+ of γδTCR+ lymphocytes (%)
r = 0.61
p = 0.001

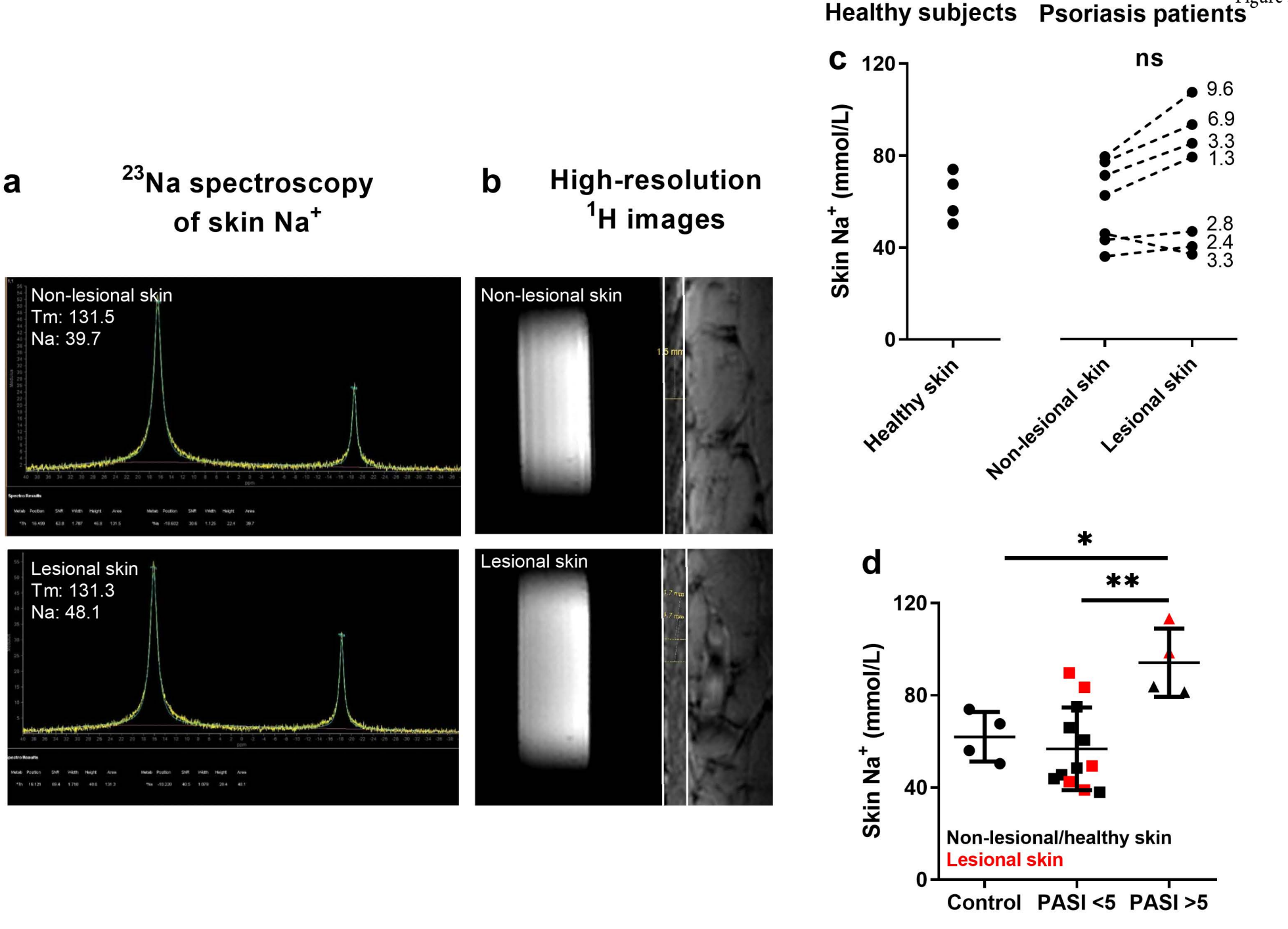
a
^{23}Na spectroscopy of skin Na$^+$
b
High-resolution ^{1}H images
Non-lesional skin
Tm: 131.5
Na: 39.7
Lesional skin
Tm: 131.3
Na: 48.1
Non-lesional skin
Lesional skin
c
Healthy subjects
Psoriasis patients
ns
Skin Na$^+$ (mmol/L)
120
80
40
0
9.6
6.9
3.3
1.3
2.8
2.4
3.3
Healthy skin
Non-lesional skin
Lesional skin
d
*
**
Skin Na$^+$ (mmol/L)
120
80
40
0
Non-lesional/healthy skin
Lesional skin
Control
PASI <5
PASI >5

Figure 4

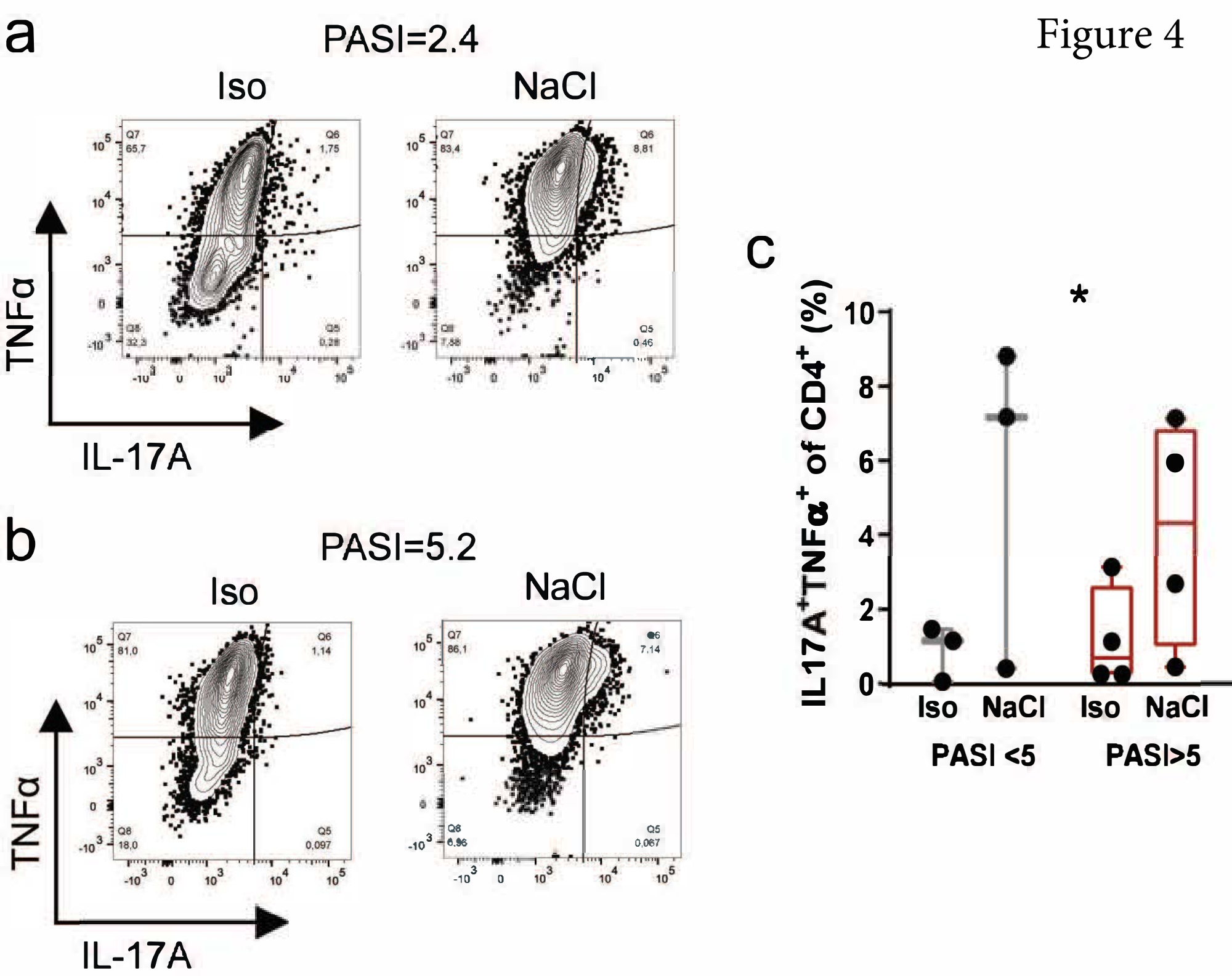
a
PASI=2.4
Iso
NaCl
Q7
65,7
Q6
1,75
Q8
32,3
Q5
0,28
Q7
83,4
Q6
8,81
Q8
7,58
Q5
0,46
TNFα
IL-17A
b
PASI=5.2
Iso
NaCl
Q7
81,0
Q6
1,14
Q8
18,0
Q5
0,097
Q7
86,1
Q6
7,14
Q8
6,96
Q5
0,067
TNFα
IL-17A
c
IL17A+TNFα+ of CD4+ (%)
*
Iso
NaCl
Iso
NaCl
PASI <5
PASI>5

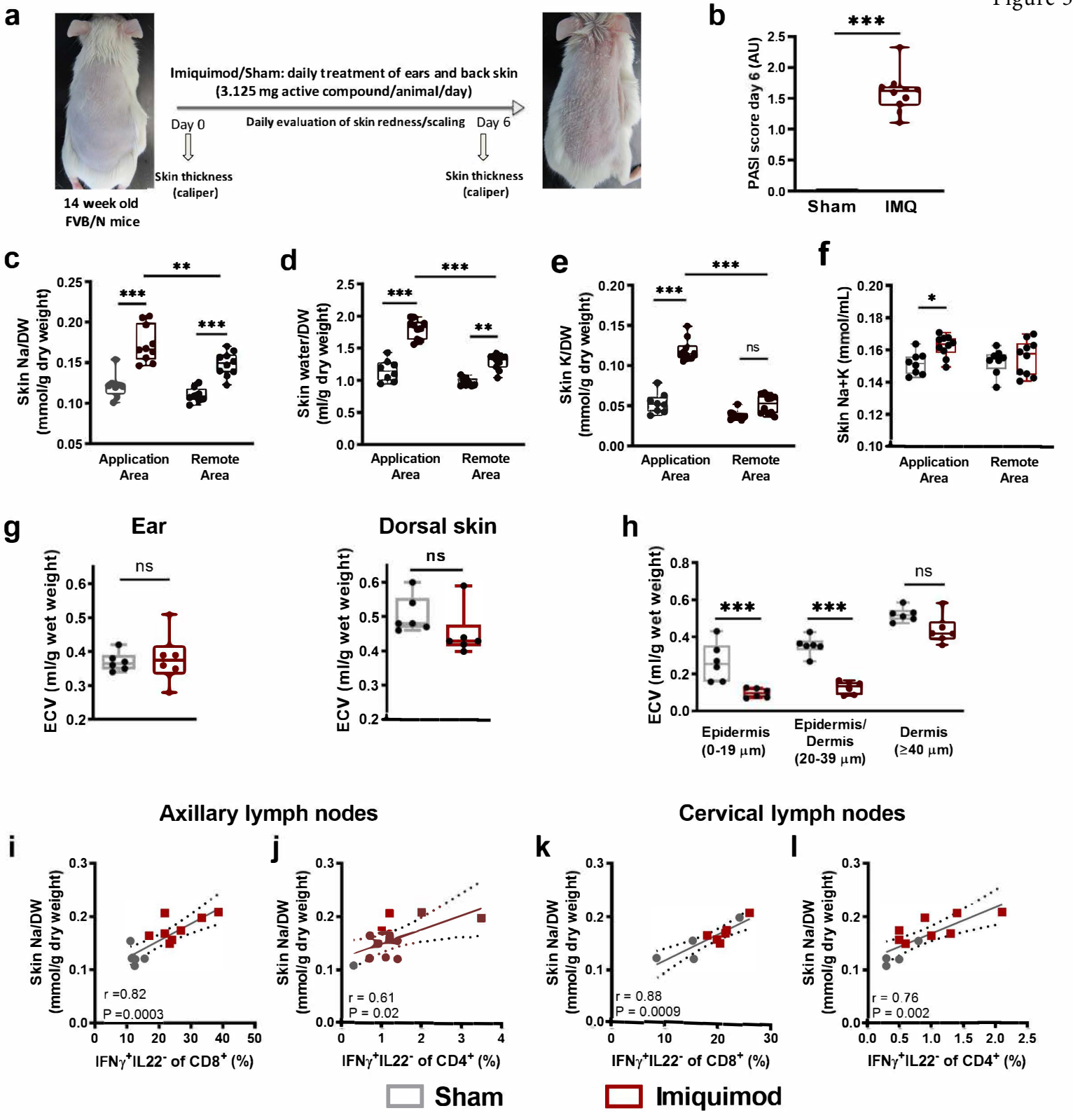
a
Imiquimod/Sham: daily treatment of ears and back skin
(3.125 mg active compound/animal/day)
Day 0
Daily evaluation of skin redness/scaling
Day 6
Skin thickness (caliper)
Skin thickness (caliper)
14 week old FVB/N mice
b
PASI score day 6 (AU)
Sham
IMQ
c
Skin Na/DW (mmol/g dry weight)
Application Area
Remote Area
d
Skin water/DW (ml/g dry weight)
e
Skin K/DW (mmol/g dry weight)
ns
f
Skin Na+K (mmol/mL)
g
Ear
Dorsal skin
ECV (ml/g wet weight)
h
Epidermis (0-19 μm)
Epidermis/ Dermis (20-39 μm)
Dermis (≥40 μm)
Axillary lymph nodes
Cervical lymph nodes
i
r =0.82
P =0.0003
IFNγ+IL22- of CD8+ (%)
j
r = 0.61
P = 0.02
IFNγ+IL22- of CD4+ (%)
k
r = 0.88
P = 0.0009
l
r = 0.76
P = 0.002
Sham
Imiquimod

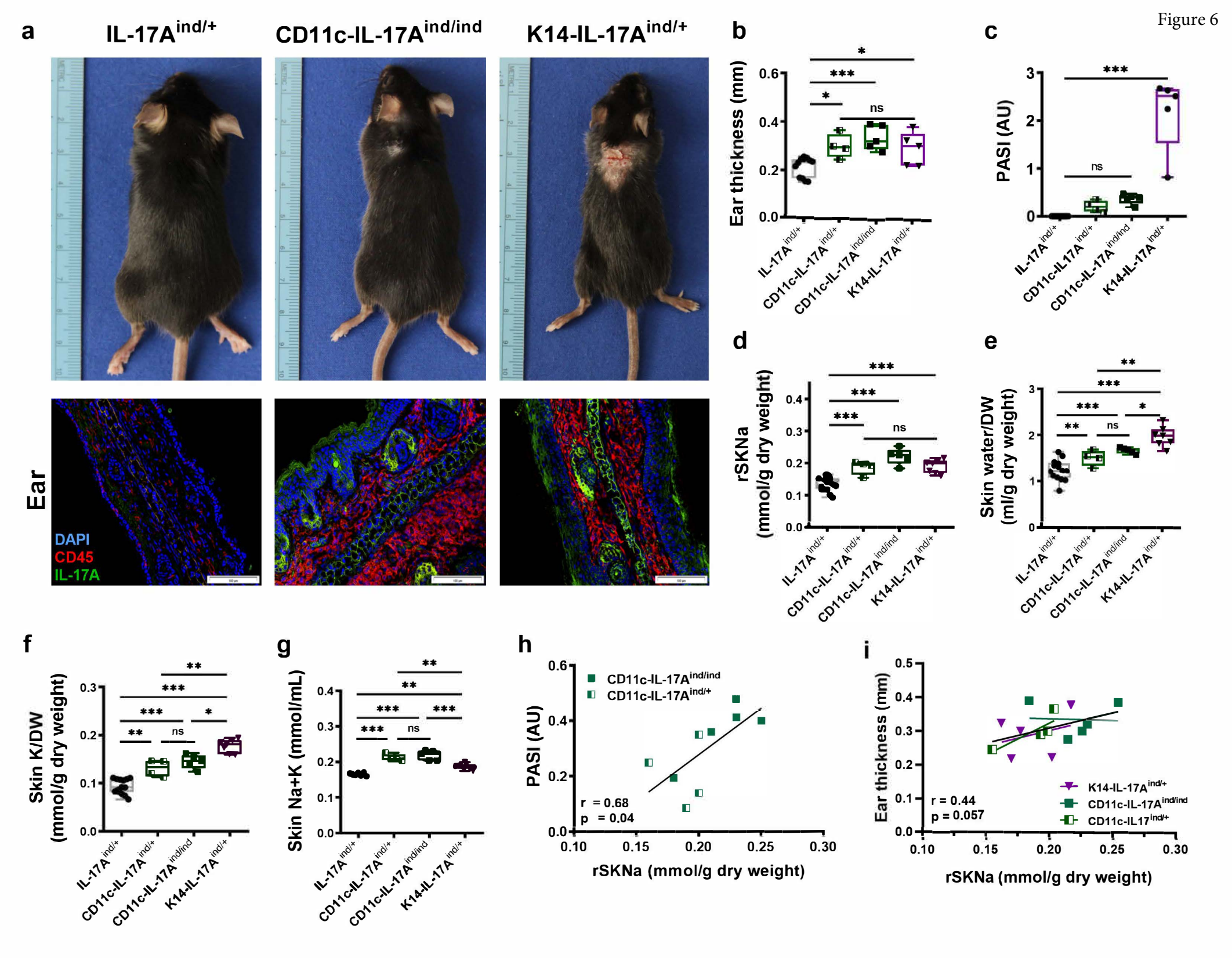
a
IL-17A ind/+
CD11c-IL-17A ind/ind
K14-IL-17A ind/+
Ear
DAPI
CD45
IL-17A
b
Ear thickness (mm)
c
PASI (AU)
d
rSKNa (mmol/g dry weight)
e
Skin water/DW (ml/g dry weight)
f
Skin K/DW (mmol/g dry weight)
g
Skin Na+K (mmol/mL)
h
PASI (AU)
CD11c-IL-17A ind/ind
CD11c-IL-17A ind/+
r = 0.68
p = 0.04
rSKNa (mmol/g dry weight)
i
Ear thickness (mm)
r = 0.44
p = 0.057
K14-IL-17A ind/+
CD11c-IL-17A ind/ind
CD11c-IL17 ind/+
rSKNa (mmol/g dry weight)

SUPPLEMETARY DATA

Skin Sodium Accumulates in Psoriasis and Reflects Disease Severity

András Maifeld[1,2,3,4]*, Johannes Wild[5,6]*, Tine V. Karlsen[7], Natalia Rakova[1], Elisa Wistorf[1], Peter Linz[8,9], Rebecca Jung[6,10], Anna Birukov[1,2,11,12], Vladimir-Andrey Gimenez-Rivera[13], Nicola Wilck[1,2,3,14], Theda Bartolomaeus[1,2,4], Ralf Dechend[1,2,3,4,15], Markus Kleinewietfeld[16], Sofia K. Forslund[1,2,3,4], Andreas Krause[17], Georgios Kokolakis[18], Sandra Philipp[18], Björn E. Clausen[9], Anna Brand[9], Ari Waisman[9], Florian C. Kurschus[19], Joanna Wegner[20], Michael Schultheis[20], Friedrich C. Luft[1], Michael Boschmann[1,3,4], Marcus Kelm[3,21,22], Helge Wiig[7], Titus Kuehne[21,22], Dominik N. Müller[1,2,3,4,23*], Susanne Karbach[5,6*], Lajos Markó[1,2,3,4*]

[1]Experimental and Clinical Research Center, a cooperation of Charité – Universitätsmedizin Berlin and Max Delbrück Center for Molecular Medicine, Berlin, Germany.

[2]DZHK (German Centre for Cardiovascular Research), partner site Berlin, Germany.

[3]Berlin Institute of Health at Charité - Universitätsmedizin Berlin, Berlin, Germany.

[4]Charité - Universitätsmedizin Berlin, corporate member of Freie Universität Berlin and Humboldt-Universität zu Berlin, Berlin, Germany.

[5]Center of Cardiology - Cardiology I, Johannes Gutenberg-University Mainz, Mainz, Germany.

[6]Center for Thrombosis and Hemostasis (CTH), Johannes Gutenberg-University Mainz, Mainz, Germany.

[7]Department of Biomedicine, University of Bergen, Norway.

[8]Institute of Radiology, Friedrich-Alexander-University Erlangen-Nürnberg, Erlangen, Germany.

[9]Department of Nephrology and Hypertension, Friedrich-Alexander-University Erlangen-Nürnberg, Erlangen, Germany

[10]Institute for Molecular Medicine, University Medical Center Mainz, Mainz, Germany.

[11]Department of Molecular Epidemiology, German Institute of Human Nutrition Potsdam-Rehbrücke, Nuthetal, Germany.

[12]German Center for Diabetes Research (DZD), München–Neuherberg, Germany.

[13]IntegraSkin GmbH i.G., Tübingen, Germany

[14]Charité - Universitätsmedizin Berlin, corporate member of Freie Universität Berlin and Humboldt-Universität zu Berlin, Department of Nephrology and Internal Intensive Care Medicine, Berlin, Germany

[15]Helios Clinic Berlin-Buch, Berlin, Germany.

[16]VIB Laboratory of Translational Immunomodulation, VIB Center for Inflammation Research (IRC), UHasselt, Campus Diepenbeek, Hasselt, Belgium.

[17]Immanuel Krankenhaus Berlin, Medical Centre for Rheumatology and Clinical Immunology, Berlin, Germany.

[18]Charité - Universitätsmedizin Berlin, corporate member of Freie Universität Berlin and Humboldt-Universität zu Berlin, Department of Dermatology, Venereology and Allergology, Berlin, Germany

[19]Department of Dermatology, Heidelberg University Hospital, Heidelberg, Germany

[20]Department of Dermatology, University Medical Center Mainz, Mainz, Germany

[21]Institute for Imaging Science and Computational Modelling in Cardiovascular Medicine, Charité - Universitätsmedizin Berlin, Berlin, Germany

[22]Department of Congenital Heart Disease, German Heart Center Berlin (Deutsches Herzzentrum Berlin, DHZB), Berlin, Germany.

[23]Max Delbrück Center for Molecular Medicine in the Helmholtz Association Berlin, Germany.

* These authors contributed equally to this work

Corresponding author: Lajos Markó, Experimental and Clinical Research Center, a cooperation of Charité - Universitätsmedizin Berlin and Max Delbrück Center for Molecular

Medicine, Lindenberger Weg 80, 13125 Berlin, Germany. Phone: +49-30-450-540-144. Email: lajos.marko@charite.de.

Short title: Skin Sodium in Psoriasis

Supplementary Methods

Studies with psoriasis patients and healthy controls

Inclusion criteria were age 18–80 years, a body mass index between 18.5 and 40 kg/m^2 and glomerular filtration rate >60 ml/min/1.73m^2. Exclusion criteria were diagnosed or treated hypertension and/or blood pressure above 140/90 mmHg at screening, palpable peripheral edema by physical examination, any type of diabetes mellitus and/or HgbA1c>6.5% at screening, subjects with a thyroid-stimulating hormone >4.2 mU/L at screening, psoriasis patients treated with systemic corticosteroids, chemotherapy agent (methothrexate) or with any kind of biologics/biosimilars (only systemic treatment allowed was dimethyl fumarate; therapy modalities in groups of patients with PASI lower or higher than 5 are shown in Supplemental Table 2), subjects with acute disease, pregnant or lactating women, subjects with metal or medical device implant in the body, subjects with tattoos on the lower extremities, subjects with a history of drug or alcohol abuse and subjects who were legally incapacitated or whose circumstances did not enable the patient to fully understand the nature, significance and scope of this study. Psoriasis patients were recruited from the Department of Dermatology, Venereology and Allergology Charité – Universitätsmedizin Berlin, from the Immanuel Hospital Berlin-Buch and from the Helios Hospital Berlin-Buch. Healthy volunteers were recruited from the Experimental and Clinical Research Center (ECRC), Berlin, Germany or were volunteering family members of psoriasis patients. The study – excluding MRI measurements - was conducted at the ECRC. MRI measurements were performed at the Magnetic Resonance Imaging Department of the German Heart Institute Berlin. MRI measurements were performed usually the same day (in case of physical examination and blood test was performed in the morning and, when included, MRI measurements late afternoon) or within maximum of 5 days after screening. PASI was assessed by a single medical doctor (LM) through the study to avoid inter-observer variability.

^{23}Na-MRI estimation of skin Na^{+} content in humans

All subjects rested for at least 15 min before their left calf was scanned at its widest circumference. Imaging was performed on a Philips Ingenia 3.0 Tesla MR scanner (Ingenia R 5.4, Philips Healthcare, Best, The Netherlands) using a transmit/receive birdcage ^{23}Na knee-coil (Rapid Biomedical, Rimpar, Germany) and a 3D-spoiled gradient echo sequence (total acquisition time, TA = 20.5 min; echo time, TE = 2.07 ms; repetition time, TR = 100 ms; flip angle, FA = 90°; 196 averages, resolution: 3 × 3 × 30 mm^3). Four calibration phantoms containing aqueous solutions of 10, 20, 30, and 40 mmol/L NaCl were scanned as reference standards, together with the subject's calf. Simultaneously, tissue water content was measured by ^{1}H-MRI, using a fat-saturated inversion-prepared SE sequence (inversion time, TI = 210 ms; TA = 6.27 min; TE = 12 ms; TR = 3000 ms ;FA = 90°; 1 average, resolution: 1.5 × 1.5 × 5 mm^3). The Na-MRI grayscale measurements of aqueous standard solutions with increasing Na^+ concentrations served to calibrate relative tissue Na^+. Images were analysed independently by two researchers (ABi and LM). The intraclass correlation coefficient (calculated form the between-groups mean square, the within-groups mean square, and the number of subjects in each group) was an excellent of 0.89.

^{23}Na-spectroscopy of skin Na^{+} content in humans

A custom-made double-resonant ^{1}H/^{23}Na-surface coil (Stark-Contrast, Erlangen, Germany) for high resolution imaging and sodium spectroscopy of human lower leg skin was implemented at the same 3.0 Tesla MR-scanner. The coil consists of a 1 cm diameter ^{23}Na-loop, a concentric 3.5 cm diameter ^{1}H-loop and a 100 mM NaCl reference solution. A shift reagent (50 mM Tm[DOTP]^{5}, Macrocyclics, Dallas, USA) was added to the solution to shift the resonance peak of the internal reference 35-40 ppm relative to the center-frequency of the skin-peak, which allow for discrimination of ^{23}Na from reference and skin using a free induction-decay sequence.

High resolution axial slices were acquired by a ^{1}H-FISP-sequence: field of view = 66 mm, base resolution = 512, slice thickness = 2 mm, number of slices = 5, TR = 196 ms, TE = 9.84 ms, TA = 1 min, FA = 90° and BW = 130 Hz/Px. The in-plane resolution was doubled by a single interpolation within the reconstruction of the MRI-raw data set to a final value of 64 µm per pixel. Skin thickness was defined by densitometry (NIH, ImageJ 1.50i) from these images as half increase of signal between the fat – dermal intersection on the one side and the epidermal – extracorporal intersection on the other. Knowledge about skin sodium content together with the thickness of the dermal layer and area of acquisition allows for determining the local skin sodium concentration. The calculation assumed that the subcutaneous fat contains negligible amount of sodium.

PASI scoring in mouse models

Erythema and scaling were scored (score range 0-4). Skin thickness was quantitatively measured using a dial thickness gage (Mitutoyo, ModelNr.: 7326, USA, and the percentage of affected skin was determined. Cumulative PASI score of the K14-IL-17A$^{ind/+}$ and the CD11c-IL-17A$^{ind/ind}$ mice was calculated as follows: *(erythema score + scaling score + skin thickness change [%]) x affected area [%]*. In IMQ experiments, percentage of affected skin is not included in the overall scoring because it depends on the treated area. Here, the modified PASI is calculated as *erythema score + scaling score + skin thickness change (%)*. In the figures, either the cumulative PASI score and/or the single scores for skin thickness, scaling, and erythema are presented.

Flow cytometric analysis of human PBMCs

Peripheral venous blood was sampled and peripheral blood mononuclear cells were isolated within 4 hours by density gradient centrifugation using Biocoll (Merck, Darmstadt, Germany) and cryopreserved until further processing. From thawed aliquots of the samples CD4^{+} and

$CD4^-$ cell fractions were selected by Miltenyi $CD4^+$ Selection Kit according to the instructions of the manufacturer. 10^6 cells from $CD4^+$ and $CD4^-$ fractions were placed onto 96-well U-bottom plates and re-stimulated for 4 hours in the presence of 50 ng/ml PMA (Sigma), 250 ng/ml ionomycin (Sigma) and 1.3 µl/ml Golgistop (BD) at 37°C and 5% CO_2 in a humidified incubator in a final volume of 200 µl RPMI 1640 (Sigma) supplemented with 10% FBS (Merck), 100 U/ml penicillin (Sigma), 100 mg/ml streptomycin (Sigma). Re-stimulated cells were labelled with Aqua Life/Dead Viability Staining kit (Invitrogen) in order to discrimination between dead and viable cells. Furthermore, surface labelling was performed using the respective fluorophore-conjugated anti-human antibodies (CD3, PerCP-Vio700, clone: BW264/56, Miltenyi, γδTCR, PE, clone: 11F2, Miltenyi), followed by fixation and permeabilization by FoxP3/Transcription Factor Staining Kit (eBioscience). Cells were subsequently labelled with the respective intracellular-human-specific fluorophore-conjugated monoclonal antibodies (IFNg, PE-Vio770, clone: 45-15, Miltenyi, IL17A, APC-Vio770, clone: CZ8-23G1, Miltenyi). Samples were analyzed using FACSCanto II multicolor flow cytometer (BD). Data analysis was performed with FlowJo 10.3 (FlowJo LLC) software.

Stimulation of human cells

Cryopreserved PBMC aliquots containing 10^7 cells of psoriasis patients were thawn on 37°C water bath, washed and followed by the subsequent isolation of naïve $CD4^+$ T cells using Miltenyi CD4 Naive Kit II according to the manufacturer´s protocol. 50.000 naïve $CD4^+$ enriched cell fractions per well were polarized under Th17- polarizing conditions under isotonic conditions or in the presence of +40 mM NaCl seven days long. Briefly, cells were plated onto a-CD3-coated (10 µg/ml, NALE, BD) Costar U-well plates (Corning) in a final volume of 200 µl in the presence of the following cytokines and antibodies TGFβ (5 ng/ml), IL-1β (12.5 ng/ml), IL-6 (25 ng/ml), IL-23 (25 ng/ml), IL-21 (25 ng/ml), a-IFNγ (10 µg/ml, BD), a-IL-4 (10 µg/ml, BD) (all Miltenyi) and a-CD28 (1 µg/ml, BD) in X-Vivo15 medium (BioWhittaker).

On day seven cells were restimulated with phorbol 12-myristate 13-acetate (250 ng/ml, Sigma) and ionomycin (100 ng/ml, Sigma) in the presence of GolgiStop containing monensin (2 µl/3ml, BD) 4 hours long. Cells were subsequently stained for live/dead exclusion with Viability Stain 700 dye (Biolegend), permeabilized with FoxP3 Transcription Buffer Kit (eBioscience), and stained with the following antibodies a-Helios FITC (clone 22F6, 2:100, Biolegend), a-FoxP3 BB700 (clone 236A/E7, 5:100, BD), a-IL-22 Vio667 (clone REA 466, 1:100, Miltenyi), a-CD4 APC-Vio770 (clone REA623, 4:100, Miltenyi), a-TNFα BV750 (clone MAb11, 5:100, BD), a-IL10 BV711 (clone JES-9D7, 5:100, BD), a-Ki-67 BV650 (clone B56, 2.5:100, BD) a-IFNγ BV605 (clone B27, 5:100, BD), a-IL-17A BV510 (clone N49-653, 5:100, BD), a-IL-13 BV421 (clone JES10-5A2, BD), a-GM-CSF PE-Vio770 (clone REA1215, 2:100, Miltenyi), a-CD3 PE-Cy5 (clone UCHT1, 10:100, BD), a-IL-9 PE-CF594 (clone MH9A3, 5:100, BD), a-IL-5 PE (clone JES1-39D10, 10:100, Miltenyi). Cells were analyzed on LSR-Fortessa multicolor flow cytometer platform (BD) with Diva 8.0.2 (BD) and FlowJo 10.6.2 software (BD).

Flow cytometric analysis of spleens and regional lymph nodes of mice

Spleens and lymph nodes were isolated from mice and minced through 40 µm cell strainer to obtain single cell solutions. Red blood cell lysis was performed for spleen samples using ACK lysis buffer (1.5 M NH_4Cl, 100 mM $KHCO_3$, 10 mM EDTA-2Na). An equal number of cells was plated and unspecific Fc-receptor binding was blocked by the incubation with anti-CD16/CD32. For the assessment of the cytokine production of the cells, cells were stimulated prior to Fc-blocking and staining for 4 h at 37 °C with Phorbol 12-myristate 13-acetate (PMA, 50 ng/ml) and Inonmycin (500 ng/ml) in T cell medium (RPMI 1640 medium with 10% FCS (v/v), 1mM sodium pyruvate, 2 mM L-glutamine, 1 x Non-essential Amino Acid Solution, 1% (v/v) penicillin/streptomycin, 10 mM HEPES and 0.1 mM 2-mercaptoethanol). Brefeldin A (1 µg/ml) was added as a Golgi-Stop. After the incubation cells were washed and stained with Aqua Life/Dead Viability Staining kit (Invitrogen) in to discriminate between dead and viable

cells. Subsequently, cells were stained with fluorophore-coupled antibodies (CD3, eFluor660, clone: 17A2; TCR-γδ, PE, clone: eBio GL3; CD4, Pacific Blue, clone: RM4-5; CD4, APCCy7, clone: RM4-5; CD90.2 Pacific blue, clone: 53-2.1; CD8, PerCP, clone: 53-6.7; CD8, PE-Cy7, clone: 53-6.7; fixable viability dye, eFluor™ 506, LIVE/DEAD fixable viability dye near-infrared). For the intracellular staining, cells were permeabilized with the BD Cytofix/Cytoperm™kit or with FoxP3/Transcription Factor Staining Kit (eBioscience) and stained with anti-IL-17A, APC, clone: eBio17B7; anti-IFNγ PE-Cy7, clone: XMG1.2, PerCP-Cy5.5, cline XMG1.2; anti-IL-22, PE, clone: 1H88WSR. The acquisition of stained cells was conducted with the FACS™ Canto II cytometer (BD) and final analysis was performed with FlowJo software (BD).

Histology and immunohistology

To measure dorsal and ventral skin thickness in the IMQ model we took skin biopsies from the same area of the mouse skin, fixed in 5% formalin and embedded them in paraffin. Paraffin blocks of skin biopsies were prepared using routine methods and 2 µm sections were made. The sections were haematoxylin and eosin stained and thickness of epidermis and dermis was measured by averaging at least 5 different areas. Eight µm cryosections of ear skin were stained with fluorophore-coupled antibodies against IL-17A (clone: TC11-18H10.1, BioLegend) and CD45.2 (clone: 104, eBioscience). DAPI staining was conducted subsequently.

Measurement of electrolyte and water content in mouse skin

Briefly, complete (except small biopsy for histology) dorsal and ventral skin of mouse carcasses were collected. Skin was weighted (wet weight) and then desiccated both at 90°C for 72 hours (dry weight [DW]). Because weights were unchanged with further drying, the difference between wet weight and DW was considered as tissue water content. Dried skin was ashed at 190°C for 5 hours, at 300 °C for another 5 hours and finally at 450°C for 11 hours excluding 1

hour to ramp up the temperature between each step (total of 24 hours of ashing). Ash was dissolved in 5% HNO_3 and Na^+ and K^+ concentrations were measured by atomic adsorption spectrometry (Model AAnalyst200, Perkin Elmer).

Measurement of extracellular volume in skin and ears

Skin extracellular volume was determined by assessing the extracellular distribution volume of the tracer ^{51}Cr-EDTA (produced by GE Healthcare Limited; delivered by IFE, Institute for Energy Technology, Kjeller, Norway). Imiquimod-treated and control mice were anesthetized with 1.5% isoflurane (IsoFlo®Vet 100%; Abbott Laboratories Ltd, Maidenhead, UK) in 100% O_2 before the kidney pedicles were ligated to prevent tracer escape during the experiment. Body temperature was kept at 37°C throughout the experiment with the aid of a servo-controlled heating pad. The ^{51}Cr-EDTA tracer (5 mill cpm in 0.1 ml isotonic saline) was injected i.v. into the tail vein and allowed to distribute for 60 min before a terminal blood sample was collected by cardiac puncture. The mice were sacrificed by cervical dislocation before ears and two back skin samples were harvested. From each mouse, one snap-frozen back skin sample with the epidermis facing up was cut into 20 µm consecutive horizontal sections using a freezing slide microtome. Back skin sections, intact back skin, ears and a plasma samples were weighed and counted in a gamma counter. The extracellular volume of skin was calculated as the plasma equivalent space of ^{51}Cr-EDTA: (^{51}Cr-EDTA counts/g tissue)/ (^{51}Cr-EDTA counts/ml plasma).

Statistical analysis

Data were tested for normal distribution (Kolmogorov-Smirnov test). In case of normal distribution, unpaired t-test (in case of two groups) or one-way ANOVA (in case of more than two groups) with Bonferroni post hoc test was applied. In case of non-normal distribution, Mann-Whitney test (in case of two groups) or Kruskal-Wallis test (in case of more than two groups) with Dunn's multiple comparison test or comparison of selected columns as

appropriate and indicated in the figure legends. Two-way ANOVA with Bonferroni's multiple comparisons test were performed where two different categorical independent variables was tested on one continuous dependent variable (e.g. IMQ/Sham treatment and creamed/not creamed area on electrolyte content). To evaluate correlations between 2 variables Pearson correlation coefficients were calculated. Fisher’s exact test was used to compare dichotomous variables.

Supplementary Figure 1.

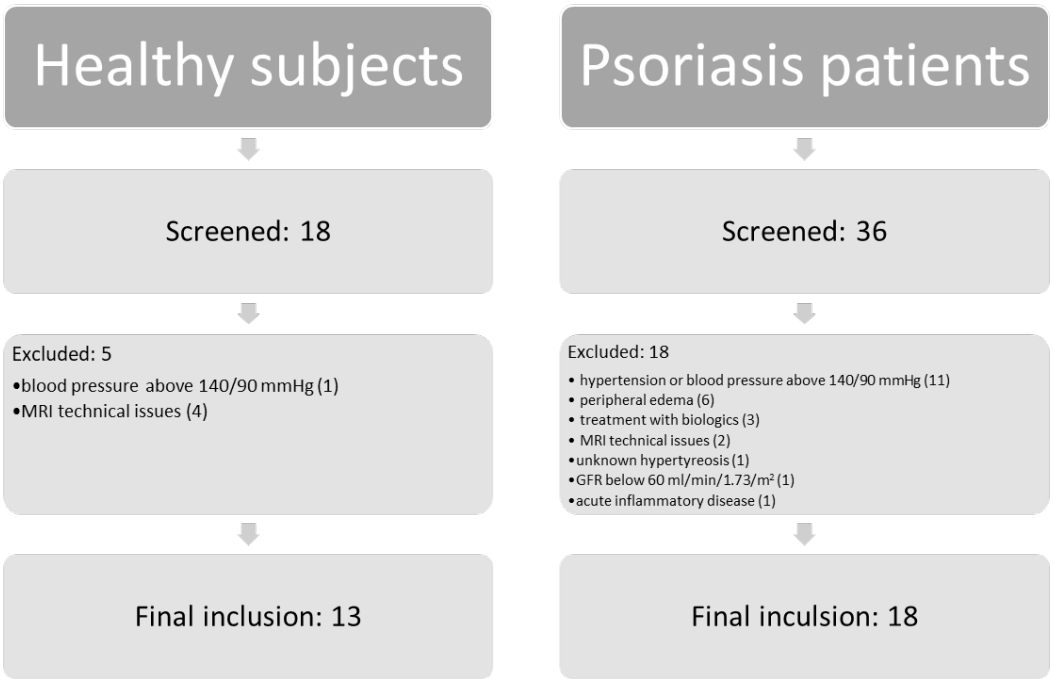

Supplementary Figure 1. Flow chart of the number of healthy subjects and psoriasis patients screened, excluded (showing the reason for exclusion and in parenthesis the number of patients) and finally included in the study. Please note that in case of in 7 cases psoriasis patients more than one exclusion criteria were present but counted separately.

Supplementary Figure 2.

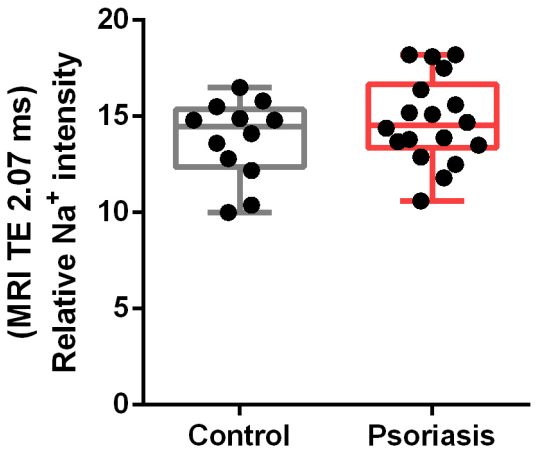

Supplementary Figure 2. Skin sodium content in healthy control and psoriasis patients measured by ^{23}Na MRI. Relative Na^+ intensity in the skin of healthy controls and in unstratified psoriasis patients.

Supplementary Figure 3.

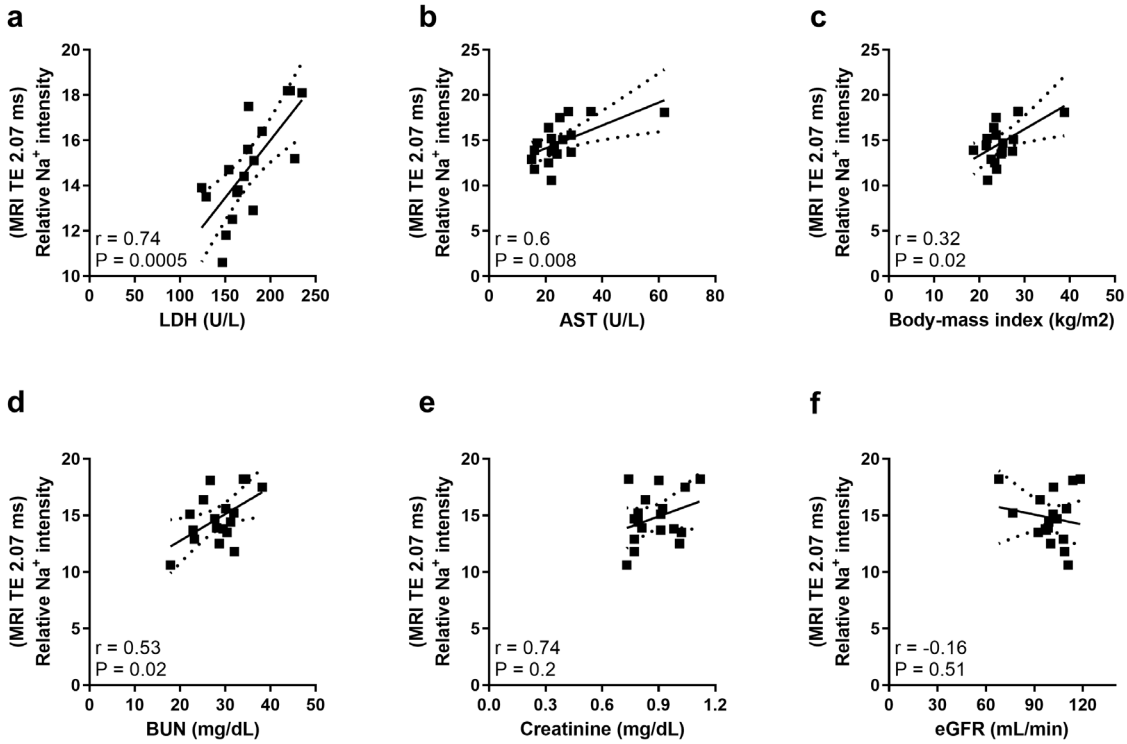

Supplementary Figure 3. Correlations of skin sodium content of psoriasis patients measured by ^{23}Na MRI correlates with laboratory parameters. Relative Na^+ intensity in the skin of psoriasis patients (n=18) significantly and positively correlated with blood (a) lactate dehydrogenase levels, (b) aspartate transaminase levels, (c) body mass index, (d) blood urea nitrogen concentrations, (e) but not with serum creatinine or (f) estimated (using Chronic Kidney Disease Epidemiology Collaboration equation) glomerular filtration rates. Pearson correlation coefficient (r) was calculated and p value (two-tailed) reported.

Supplementary Figure 4

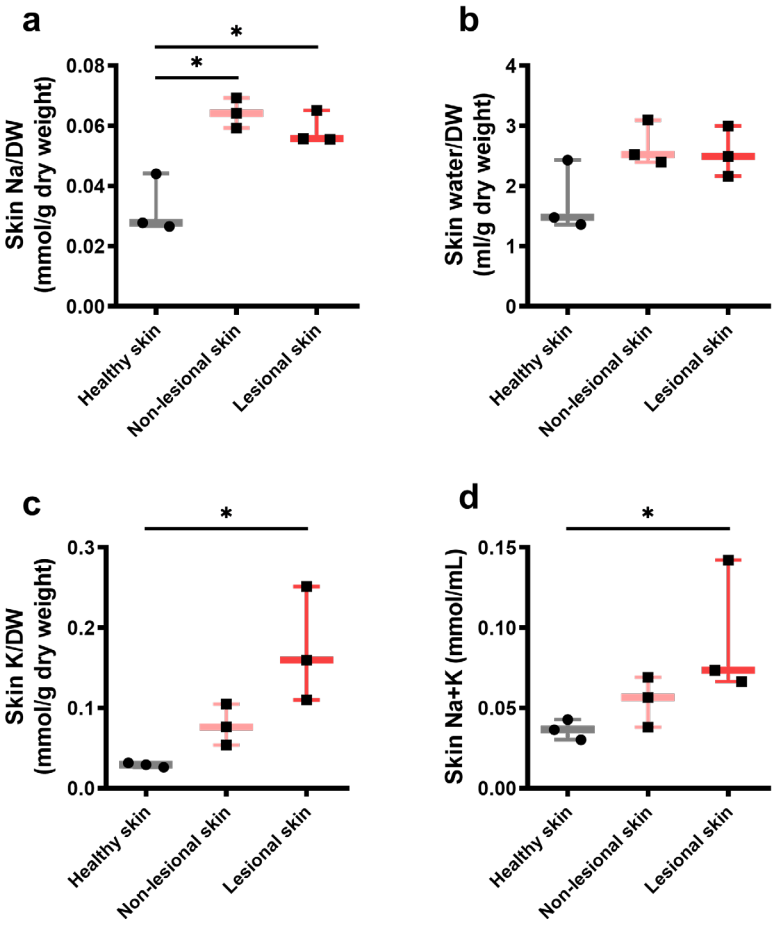

Supplementary Figure 4. Skin sodium, potassium and water content and odium plus potassium concentration in skin of healthy control and psoriasis patients with PASI>5 measured by atomic adsorption spectrometry. (a) Sodium (b) water and (c) potassium content and (d) sodium plus potassium concentration of the skin of healthy controls and in patients with PASI>5. *P < 0.05.

Supplementary Figure 5.

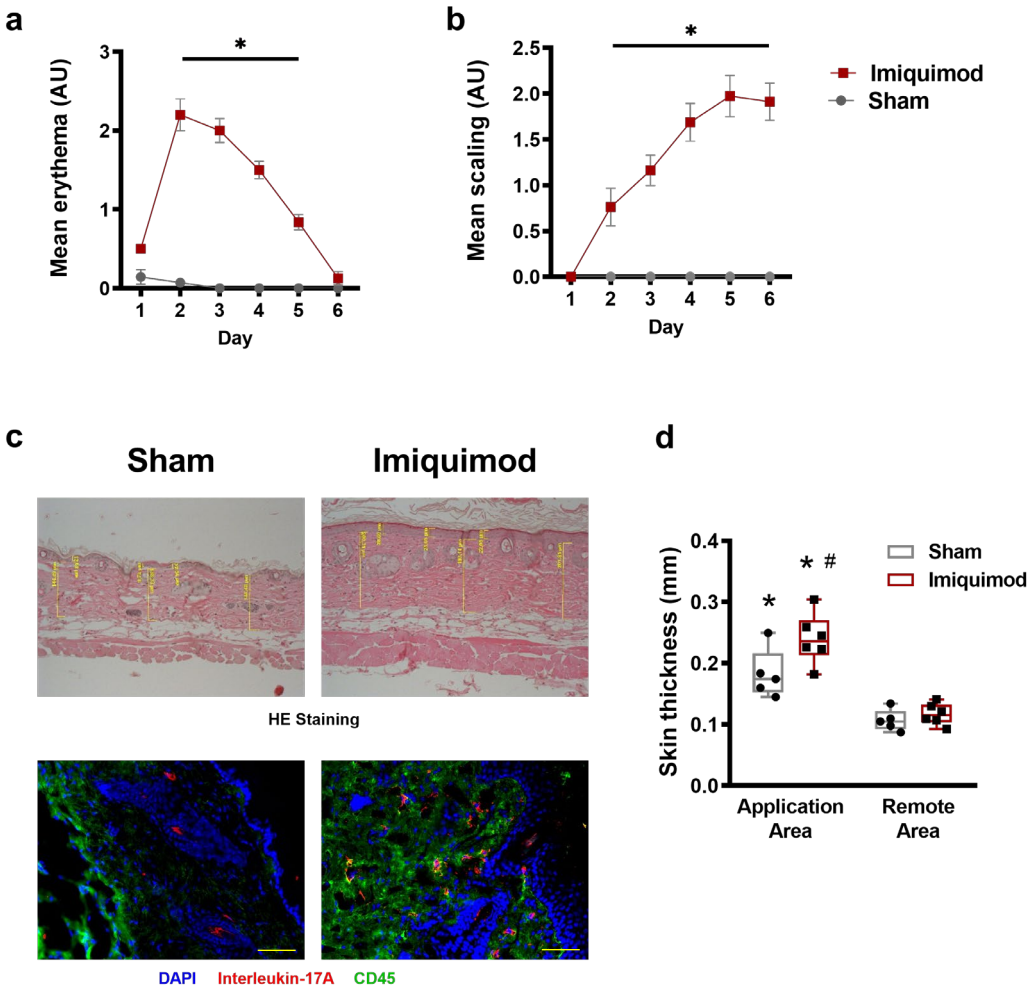

Supplementary Figure 5. Characterisation of the mouse (IMQ)-induced psoriasis-like skin disease model. (a) Daily mean erythema and (b) scaling scores of sham (n=7) or IMQ-treated mice (n=10). *P<0.05, two-way repeated measures ANOVA followed by Bonferroni's multiple comparisons test. (c) Hematoxylin and eosin (HE) staining of sham and IMQ-treated dorsal skin with epidermis and dermis thickness measurements (upper panel) and immunostaining of sham and IMQ-treated dorsal mouse skin (red: IL-17A; green: CD45.2; blue: DAPI). Scale bar = 100 µm. (d) Dorsal (application area) and ventral (remote area) skin thickness of sham (n=5) and IMQ-treated (n=6) mice as measured on HE stained sections. *P<0.01 vs sham and imiquimod remote area, #P<0.05 vs. sham application area, two-way ANOVA followed by Bonferroni's multiple comparisons test.

Supplementary Figure 6

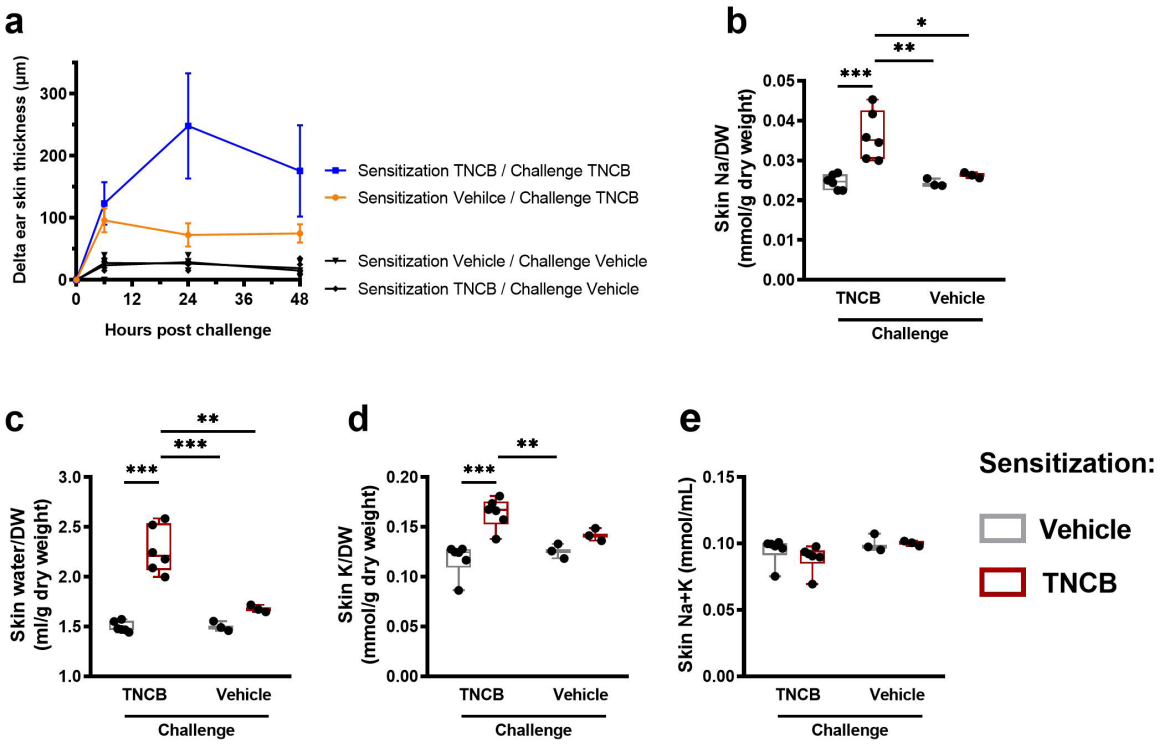

Supplementary Figure 6. Skin electrolyte and water content in the TNCB-induced allergic contact dermatitis model. (a) Changes of ear skin thickness in previously abdominally TNCB (n=6) or vehicle sensitized mice (n=3) and after challenging the ears of all mice with TNCB (right ear) or vehicle (left ear of the same mouse). (b) Sodium, (c) water (d) potassium content and (e) sodium plus potassium to water ratio of vehicle (grey boxes) or TCNB (red boxes) previously abdominally sensitized mice challenged either with TNCB (right ear) or vehicle (left ear of the same mouse). ***P < 0.001; **P < 0.01; *P<0.05, two-way ANOVA followed by Bonferroni's multiple comparisons test.

Supplementary Figure 7.

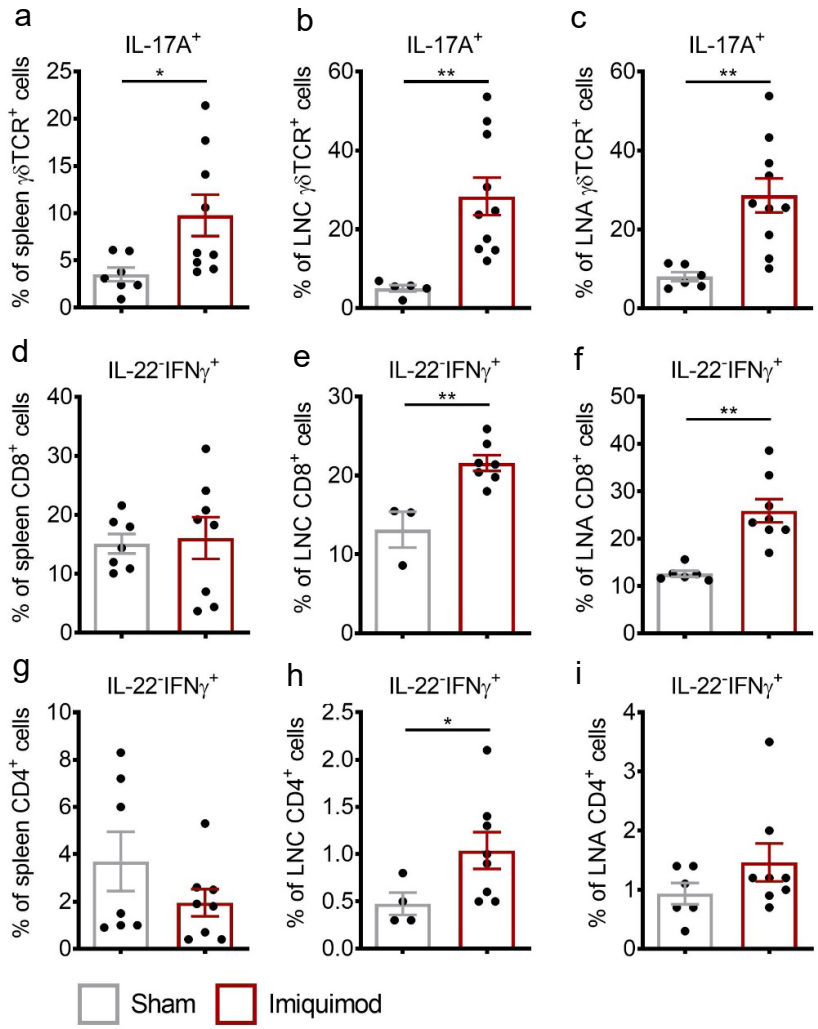

Supplementary Figure 7. Flow cytometric analysis of spleen and draining lymph nodes of sham and imiquimod (IMQ)-treated mice. IMQ-treated mice had elevated IL-17A-producing γδ TCR$^+$ cell levels in (a) the spleen (b) cervical lymph nodes (LNC) and (c) axillary lymph nodes (LNA) compared to sham mice. Th1 cell population defined as IL-22$^-$IFNγ$^+$ cells of CD8$^+$ were similar (d) in the spleen, but elevated in (e) LNC and in (f) LNA of IMQ-treated mice in comparison to sham mice; the same applied to CD4$^+$ IL-22$^-$IFNγ$^+$ cells of the (g) spleen, (h) LNC though (i) CD4$^+$ IL-22$^-$IFNγ$^+$ cells in LNA did not reach statistical significance. Sham mice n=3-7 (depending on tissue investigated) and IMQ-treated mice n=8-9 (depending on tissue investigated). Figure scatter plots indicate mean ± SD. **P < 0.01, *P < 0.05. Data analysis by unpaired t-test or Mann-Whitney U-test as appropriate.

Supplementary Table 1. Clinical characteristics of healthy subjects and psoriasis patients.

		Healthy subjects (n=12)		Psoriasis patients (n=18)		Unpaired t-test or Fisher's exact test
Parameter	**Unit**	**Mean**	**SD**	**Mean**	**SD**	**P-value**
Age	years	41.9	14.3	37.6	14.2	0.44
Gender	% male	50	n.a.	63.0	n.a.	0.71
Smoker	% yes	25	n.a.	27.8	n.a.	1.00
BMI	kg/m2	23.9	3.7	25.0	4.4	0.48
Sys BP	mmHg	120.7	10.2	118.7	11.7	0.65
Dias BP	mmHg	77.4	8.7	76.4	8.1	0.77
HF	beats/min	65.1	6.6	67.6	7.3	0.36
PVR	s*mmHg/mL	1.2	0.1	1.2	0.1	0.79
PWV	m/s	6.5	1.6	6.0	1.4	0.41
GGT	U/L	22.1	11.3	26.6	20.6	0.51
AST	U/L	23.1	4.1	25.2	10.3	0.52
ALT	U/L	19.6	7.8	29.0	30.6	0.32
LDH	U/L	173.3	22.2	176.1	31.5	0.80
Creatinine	mg/dL	0.9	0.1	0.9	0.1	0.90
BUN	mg/dL	30.8	8.1	28.6	4.9	0.38
GFR	ml/min/1.73m2	94.3	10.9	99.9	12.0	0.21
Sodium	mmol/L	141.3	1.5	142.1	2.2	0.34
Potassium	mmol/L	4.5	0.4	4.3	0.4	0.44
Chloride	mmol/L	100.9	1.8	100.7	2.0	0.80

Calcium	mmol/L	2.4	0.1	2.4	0.1	0.24
Hemoglobin	g/dL	13.9	1.0	14.4	1.0	0.17
Leucocytes	G/L	6.6	2.2	5.9	1.4	0.31
Neutrophils	G/L	4.2	2.0	3.3	1.3	0.17
Thrombocytes	G/L	250.8	52.5	219.3	47.8	0.11
hsCRP	mg/L	0.9	1.1	1.1	1.6	0.62
HbA1c	%	5.3	0.3	5.3	0.2	0.93
TSH	mU/L	1.9	0.6	1.9	0.7	0.90

Abbreviations: BMI = body mass index, BP = blood pressure, HR = heart rate, PVR = peripheral vascular resistance, PWV = pulse wave velocity, GGT = gamma-glutamyltransferase, AST = aspartate transaminase, ALT = alanine transaminase, LDH = lactate dehydrogenase, BUN = blood urea nitrogen, GFR = glomerular filtration rate, hsCRP = high sensitivity C-reactive protein, HbA1c = hemoglobin A1c, TSH = thyroid-stimulating hormone. n.a.=not applicable.

Supplementary Table 2. Treatment modalities of psoriasis patients stratified by disease activity.

	Psoriasis patient PASI<5 (n=13)	**Psoriasis patient PASI>5 (n=5)**
	% yes	**% yes**
Nail psoriasis	38.5	0.0
Psoriatic arthritis	0.0	20.0
Therapy	53.8	80.0
Local therapy	61.5	80.0
Systemic therapy	7.7	40.0
Balneo-phototherapy	7.7	20.0
Urea	0.0	60.0
Salicylic acid	7.7	0.0
Polidocanol	0.0	40.0
Dithranol	0.0	0.0
Vitamin D analogues	23.1	40.0
Topical corticosteroids	61.5	20.0
Dimethyl fumarate	7.7	40.0